

Probing the M–C_{NHC} Bond and Its Effect on the Synthesis, Structure, and Reactivity of R₂MOR(NHC) (M = Al, Ga, In) Complexes

Rafał Zaremba,^{†,‡} Maciej Dranka,^{‡,§} Bartosz Trzaskowski,[†] Lilianna Chęcińska,^{*,§,§} and Paweł Horeglad^{*,†,§}

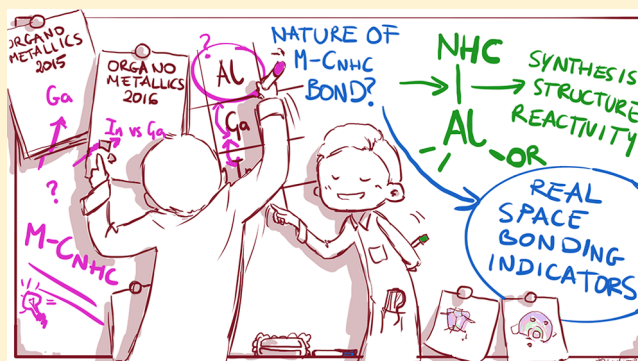
[†]Centre of New Technologies, University of Warsaw, Banacha 2c, 02-097, Warsaw, Poland

[‡]Faculty of Chemistry, Warsaw University of Technology, Noakowskiego 3, 00-664, Warsaw, Poland

[§]Faculty of Chemistry, University of Lodz, Pomorska 163/165, 90-236, Lodz, Poland

Supporting Information

ABSTRACT: The studies on the reactivity of dialkylaluminum alkoxides towards N-heterocyclic carbenes (NHCs) has allowed investigation of not only the factors controlling the synthesis and properties of Me₂AlOR(NHC) complexes. Additionally, we have focused on the effect of group 13 metals on the synthesis, structure, and reactivity of Me₂MOR(NHC) (M = Al, Ga, In) complexes, with regard to the strength and character of M–C_{NHC} bonds. The reactions of simple dimethylaluminum alkoxides with NHCs lead to the monomeric Me₂AlOR(NHC) complexes, as shown by the isolation of Me₂AlOMe(NHC) (NHC = IMes (**1a**), SIMes (**1b**)) (IMes = 1,3-bis(2,4,6-trimethylphenyl)imidazol-2-ylidene, SIMes = 1,3-bis(2,4,6-trimethylphenyl)imidazolin-2-ylidene). Despite their tendency to disproportionate, the interaction of the additional NHC molecule in Me₂Al(OCH₂CH₂OMe)(IMes)/IMes (**2a**/IMes) with the fifth coordinate site of aluminum has resulted in stabilization and allowed for the isolation of Me₂Al(OCH₂CH₂OMe)(IMes) (**2a**). In contrast, the limited accessibility of the fifth coordinate site of aluminum in the case of five-coordinate [Me₂Al(μ-OCH(Me)CO₂Me)]₂ or four-coordinate [Me₂Al(μ-OR)]₂ alkoxides with bulky alkoxide ligands, has affected the formation of Al–C_{NHC} bonds and allowed only for the synthesis and isolation of stable Me₂Al(OCPh₂Me)(NHC) (NHC = IMes (**3a**), SIMes) complexes. Additionally stable aryloxide derivatives Me₂M(OC₆H₄OMe)(NHC) (NHC = IMes (**4a**) and SIMes (**4b**)) have been isolated and characterized. More ionic Al–C_{NHC} bonds of Me₂AlOR(NHC), in comparison with analogous Ga–C_{NHC} and In–C_{NHC} bonds, have been decisive for the reactivity of aluminum complexes, which includes their tendency for ligand disproportionation and activity of **1a**, **4a**, and **4b** in the ring opening polymerization (ROP) of lactide, initiated in each case by the insertion of lactide into mainly an ionic Al–C_{NHC} bond. The ionic character of M–C_{NHC} bonds, decreasing in the series Al–C_{NHC} > In–C_{NHC} > Ga–C_{NHC}, has been reflected by the reactivity of investigated complexes and determined by density functional theory (DFT) calculations using real-space bonding indicators (RSBIs). The structure of investigated aluminum complexes and the strength of Al–C_{NHC} bonds have been investigated using spectroscopic methods and X-ray diffraction studies. The strength of M–C_{NHC} bonds of investigated aluminum complexes, as well as their gallium and indium analogues, have been also determined by DFT calculations of their bond dissociation energies.



INTRODUCTION

In recent years, main-group metal complexes with N-heterocyclic carbenes (NHCs) have become a focus of scientists, both from the point of view of fundamental studies as well as their applications in catalysis.^{1,2} In this regard, NHC-stabilized main group metal alkoxides,³ including aluminum,⁴ gallium,⁵ indium,^{5c,6} magnesium,⁷ and zinc,^{7,8} alkoxides, as well as Me₃Al(NHC)⁹ and [R₂Al(NHC)]⁺ in the presence of benzyl alcohol,¹⁰ have been shown to catalyze ring-opening polymerization (ROP) of *rac*-lactide (*rac*-LA), as well as other heterocyclic monomers, such as cyclohexyl oxide, trimethylene carbonate, and ϵ -caprolactone, in controlled and stereo-

selective fashion. Noteworthy, mentioned examples have shown that the M–C_{NHC} bond strongly influences the catalytic activity of such complexes, as demonstrated, for instance, by the high activity and stereoselectivity of heteroselective Zn alkoxides with NHCs,^{8a,c} as well as isoselective Me₂GaOR(NHC) complexes,^{5a,b} in the polymerization of *rac*-LA. Importantly, the character of M–C_{NHC} bonds was crucial for the differences between the catalytic properties of Zn and Mg complexes possessing alkoxide chelate ligands with NHC

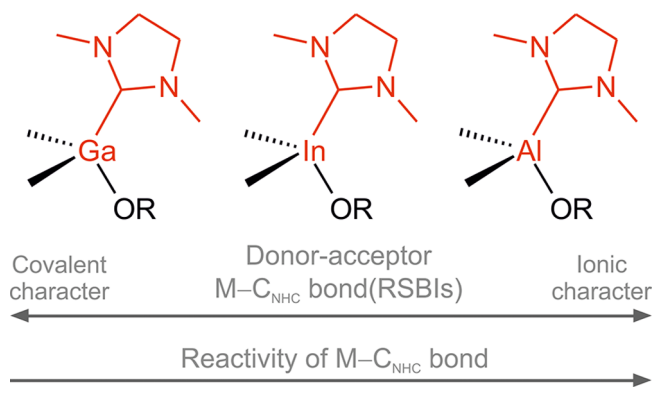
Received: August 9, 2018

termini ($O_{\text{C}_{\text{NHC}}}$), as demonstrated by Arnold et al.,⁷ while we showed its significance for $\text{Me}_2\text{GaOR}(\text{NHC})$ ^{5a,b} and $\text{Me}_2\text{InOR}(\text{NHC})$ complexes.⁶ In the former cases, insertion of lactide into the $\text{M}-\text{C}_{\text{NHC}}$ bond was indicated for Mg alkoxides in contrast to Zn alkoxides, with the $\text{Zn}-\text{C}_{\text{HNC}}$ bond remaining intact and resulting in the exclusive insertion of *rac*-LA into $\text{Zn}-\text{O}_{\text{alkoxide}}$ bond,⁷ similarly to Zn alkoxides reported by Tolman and co-workers.^{8a,c} In the case of our studies on $\text{R}_2\text{MOR}(\text{NHC})$ ($\text{M} = \text{Ga}, \text{In}, \text{NHC} = \text{IMes}, \text{SIMes}$) complexes, which are highly active and isoselective catalysts for the polymerization of *rac*-LA, we observed the insertion of *rac*-LA exclusively into $\text{Ga}-\text{O}_{\text{alkoxide}}$ bond of gallium alkoxides, while strong $\text{Ga}-\text{C}_{\text{NHC}}$ bonds remained intact during polymerization.^{5a,b} Noteworthy, even for $\text{Me}_2\text{GaOR}(6\text{-Mes})$ ($6\text{-Mes} = 1,3\text{-bis}(2,4,6\text{-trimethylphenyl})\text{-}3,4,5,6\text{-tetrahydropyrimidin-1-ylidene}$), with a much weaker $\text{Ga}-\text{C}_{6\text{-Mes}}$ bond in comparison with $\text{Ga}-\text{C}_{\text{NHC}}$ ($\text{NHC} = \text{IMes}, \text{SIMes}$), the insertion of lactide to the latter could not be evidenced.^{5c} On the contrary, in the case of $\text{Me}_2\text{InOR}(\text{NHC})$, *rac*-LA could insert under the same conditions into either an $\text{In}-\text{O}$ bond or $\text{In}-\text{C}_{\text{NHC}}$ bond, the latter considerably weaker in comparison with $\text{Ga}-\text{C}_{\text{NHC}}$ of $\text{Me}_2\text{GaOR}(\text{NHC})$.^{5c,6} Notably, the insertion of lactide into the $\text{M}-\text{C}_{\text{NHC}}$ bond was observed by Dagorne and co-workers for the ROP of lactide catalyzed with $\text{Me}_3\text{Al}(\text{NHC})$ complexes.⁹ In addition to the effect of the $\text{M}-\text{C}_{\text{NHC}}$ bond on the activity of the main group complexes in ROP, Dagorne and co-workers showed recently that changing of NHC coordination mode from normal to abnormal and vice versa, which should be expected to affect considerably the character of $\text{M}-\text{C}_{\text{NHC}}$ bond, had a profound effect on the insertion of CO_2 into either $\text{Zn}-\text{C}_{\text{NHC}}$ or $\text{Zn}-\text{Me}$ of zinc cationic complexes stabilized with NHCs.¹¹ With regard to the catalytic properties of main group metal alkoxides with NHCs, we believe that there is a need for systematic research concerning the effect of the character of $\text{M}-\text{C}_{\text{NHC}}$ bond on the structure and reactivity of main group metal alkoxides.¹² Such studies should enable researchers to understand the factors controlling reactivity of main group metal alkoxides with NHC and, as a result, rationally design new catalysts for ROP and beyond. It should also prove interesting for the synthesis of main group metal complexes with NHCs, in light of the stabilization and isolation of B,¹³ Al,¹⁴ and Ga and In complexes¹⁵ at unusual oxidation states, which have been facilitated by the formation of $\text{M}-\text{C}_{\text{NHC}}$ bonds.

With regard to the above, we have decided to investigate the effect of $\text{M}-\text{C}_{\text{NHC}}$ on the synthesis structure and reactivity, including activity in the ROP of lactide, of group 13 metal dialkylalkoxides and dialkylaryloxides with NHCs - $\text{Me}_2\text{MOR}(\text{NHC})$ and $\text{Me}_2\text{MOAr}(\text{NHC})$ ($\text{M} = \text{Al}, \text{Ga}, \text{In}; \text{OAr} = \text{aryloxy group}$) respectively. Therefore, in the first step, we have extended our studies on the synthesis, structure, and catalytic activity of $\text{Me}_2\text{MOR}(\text{NHC})$ ($\text{M} = \text{Ga}, \text{In}$)^{5c,6} complexes in ROP, to their aluminum analogues in order to determine the strength of the $\text{Al}-\text{C}_{\text{NHC}}$ bond and its effect on the synthesis structure and reactivity, including both stability and activity of aluminum complexes in the ROP of lactide. Subsequently, in order to fully determine the strength and character of $\text{M}-\text{C}_{\text{NHC}}$ ($\text{M} = \text{Al}, \text{Ga}, \text{In}$) bonds, we applied density functional theory (DFT) calculations. We hereby report the synthesis, structure, and reactivity of $\text{Me}_2\text{AlOR}(\text{NHC})$ and $\text{Me}_2\text{AlOAr}(\text{NHC})$ ($\text{NHC} = \text{IMes}, \text{SIMes}$) complexes, which constitute a barely explored class of complexes only recently reported in the literature by Camp

and co-workers.^{12h} In our case, the use of different alkoxide groups allowed us to evaluate the strength of the $\text{Al}-\text{C}_{\text{NHC}}$ bond, but also showed the considerable effect of OR and OAr groups on their synthesis and stability. With the use of both spectroscopic techniques and DFT calculations, including calculations of bond dissociation energies (BDEs) and real space bond indicators (RSBIs) of $\text{M}-\text{C}_{\text{NHC}}$ bonds, we show how the character of $\text{M}-\text{C}_{\text{NHC}}$ bonds, rather than their strength, influence the synthesis, structure, and reactivity of $\text{Me}_2\text{MOR}(\text{NHC})$ ($\text{M} = \text{Al}, \text{Ga}, \text{In}$) complexes (Scheme 1).

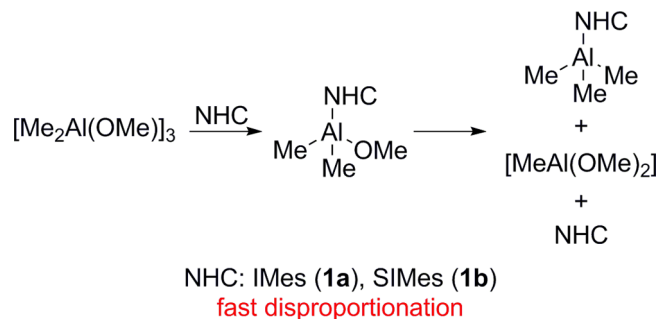
Scheme 1. Character vs Reactivity of $\text{M}-\text{C}_{\text{NHC}}$ Bond of $\text{R}_2\text{MOR}(\text{NHC})$ ($\text{M} = \text{Al}, \text{Ga}, \text{In}$) Complexes



RESULTS AND DISCUSSION

Reactivity of Simple Dialkylaluminum Alkoxides toward NHC. Dialkylaluminum derivatives $[\text{Me}_2\text{Al}(\mu\text{-OR})_n]$ ($\text{OR} = \text{OMe}, \text{OCH}_2\text{CH}_2\text{OMe}, n = 3 \text{ or } 2$) were initially selected for the reaction with NHCs, IMes and SIMes. Although NMR spectroscopy of the reaction mixtures confirmed instant formation of $\text{Me}_2\text{AlOMe}(\text{NHC})$ ($\text{NHC} = \text{IMes}$ (**1a**), SIMes (**1b**)) (Schemes 2 and 4), the observation of

Scheme 2. Synthesis and Disproportionation of $\text{Me}_2\text{AlOMe}(\text{NHC})$ ($\text{NHC} = \text{SIMes}, \text{IMes}; \text{Al}/\text{NHC} = 1:1$)



trace amounts of $\text{Me}_3\text{Al}(\text{IMes})$ and $\text{Me}_3\text{Al}(\text{SIMes})$,¹⁶ respectively, indicated that **1a** and **1b** undergo disproportionation, similar to analogues dimethylindium alkoxides with NHCs.⁶ Further decomposition of **1a** and **1b** in time led to the formation of $\text{Me}_3\text{Al}(\text{NHC})$ ($\text{NHC} = \text{IMes}, \text{SIMes}$) and a yellow crystalline precipitate. The isolated precipitate was essentially insoluble in common solvents including THF and pyridine, which precluded its further analysis. However, its general formula corresponding to $[\text{MeAl}(\text{OMe})_2]$ could be tentatively proposed.

Despite the tendency of $\text{Me}_2\text{AlOMe}(\text{NHC})$ to disproportionate, colorless crystals of **1a** and **1b**, suitable for X-ray analysis, were isolated from a toluene/hexane solution and toluene, respectively, within minutes after mixing the reagents. Similarly to $\text{Me}_2\text{GaOMe}(\text{NHC})$,^{5a,b} $\text{Me}_2\text{InOMe}(\text{SIMes})$,⁶ and $\text{Me}_2\text{InOMe}(\text{IMes})$ (see the Supporting Information), the X-ray analysis of **1a** and **1b** revealed the presence of asymmetrical aluminum complexes with the coordination sphere of aluminum of a distorted tetrahedral geometry (Figure 1).

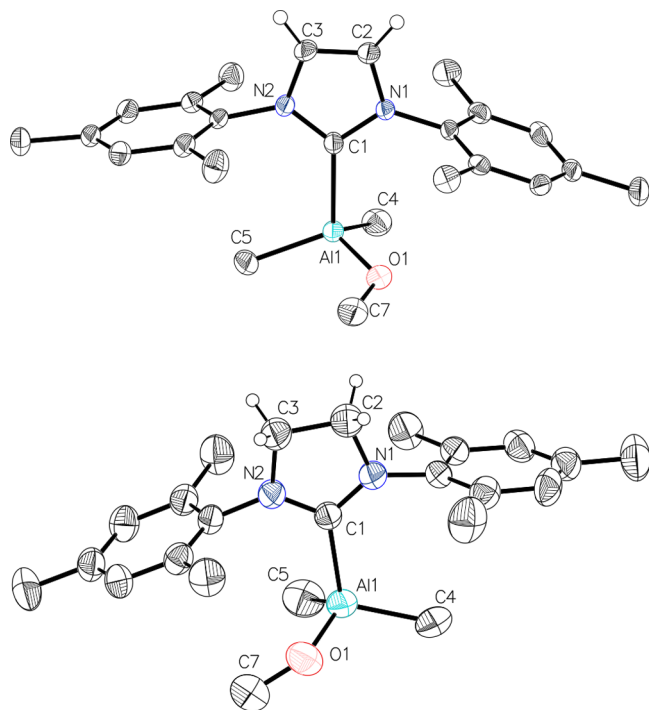


Figure 1. Molecular structure of **1a** (above) and **1b** (below) with thermal ellipsoids at the 50% probability level. Hydrogen atoms are omitted for clarity. Selected bond lengths (Å) and angles (deg) for **1a**: Al(1)–C(4) 1.983(2), Al(1)–C(5) 1.965(2), Al(1)–C(1) 2.082(2), Al(1)–O(1) 1.752(1), C(1)–Al(1)–C(4) 107.10(7), C(1)–Al(1)–C(5) 109.50(7), C(1)–Al(1)–O(1) 103.42(6), N(1)–C(1)–N(2) 103.55(12), C(5)–Al(1)–C(1)–N(1) 173.26(12), C(4)–Al(1)–C(1)–N(1) 61.95(14), O(1)–Al(1)–C(1)–N(1) 53.63(13), NHC tilt 2.0(1).¹⁷ for **1b**: Al(1)–C(4) 1.971(4), Al(1)–C(5) 1.971(5), Al(1)–C(1) 2.110(3), Al(1)–O(1) 1.746(3), C(1)–Al(1)–C(4) 108.88(16), C(1)–Al(1)–C(5) 108.63(16), C(1)–Al(1)–O(1) 104.25(14), N(1)–C(1)–N(2) 107.9(3), C(5)–Al(1)–C(1)–N(1) – 117.39(1), C(4)–Al(1)–C(1)–N(1) 5.14(1), O(1)–Al(1)–C(1)–N(1) 121.70(1), NHC tilt 4.5(1).¹⁷

The lack of symmetry was due to the orientation of the NHC ligand respective to $\text{Al}-\text{C}_{\text{Me}}$ bonds. In the case of both **1a** and **1b**, $\text{CH}\cdots\text{O}$ interactions, between the NHC heterocyclic ring and the OMe group, led to the formation of chains in the solid state, akin to those observed in $\text{Me}_2\text{MOMe}(\text{NHC})$ ($\text{M} = \text{Ga}, \text{In}$; $\text{NHC} = \text{IMes}, \text{SIMes}$).^{5a,b,6} Most importantly, the formation of strong $\text{Al}-\text{C}_{\text{NHC}}$ bonds in **1a** and **1b**, in comparison with $\text{Me}_2\text{MOR}(\text{NHC})$ ($\text{M} = \text{Ga}, \text{In}$; $\text{NHC} = \text{IMes}, \text{SIMes}$), was evidenced by the distances, and bond valencies (Table 1), of $\text{Al}-\text{C}_{\text{NHC}}$ bonds. The strength of $\text{Al}-\text{C}_{\text{NHC}}$ bonds was further evidenced by the small NHC tilts, which is split into pitch angles (out of NHC plane tilting) and yaw angles (in plane tilting),¹⁷ as well as a significant increase of NCN angles of **1a** ($103.55(12)^\circ$, $\Delta = 2.13^\circ$) and **1b**

($107.9(3)^\circ$, $\Delta = 3.19^\circ$) in comparison with free IMes ¹⁸ and SIMes ,¹⁹ respectively. The strength of the $\text{Al}-\text{C}_{\text{IMes}}$ bond in **1a** in the solid state was comparable to $\text{Ga}-\text{C}_{\text{NHC}}$ and $\text{In}-\text{C}_{\text{NHC}}$ bonds of analogous $\text{Me}_2\text{MOMe}(\text{IMes})$ ($\text{M} = \text{Ga}, \text{In}$), while the smaller ΔNCN (Table 1) of IMes upon coordination could be explained by the steric hindrances caused by a smaller radius of aluminum in comparison with gallium or indium. Interestingly, a similar valency of $\text{M}-\text{C}_{\text{IMes}}$ bonds for $\text{Me}_2\text{MOMe}(\text{IMes})$ ($\text{M} = \text{Al}, \text{Ga}, \text{In}$) complexes was surprising in the light of our recent work, which revealed significantly weaker $\text{In}-\text{C}_{\text{NHC}}$ in comparison with $\text{Ga}-\text{C}_{\text{NHC}}$ bonds in the case of $\text{Me}_2\text{MOMe}(\text{NHC})$ ($\text{M} = \text{Ga}, \text{In}$; $\text{NHC} = \text{IMes}, \text{SIMes}$). However, in the case of **1b**, the strength of $\text{Al}-\text{C}_{\text{SIMes}}$ bond in the solid state was comparable to the analogous $\text{In}-\text{C}_{\text{SIMes}}$ bond of unstable $\text{Me}_2\text{InOMe}(\text{SIMes})$ and significantly weaker in comparison with $\text{Ga}-\text{C}_{\text{SIMes}}$ bond of stable $\text{Me}_2\text{GaOMe}(\text{SIMes})$ (Table 1). Noteworthy, the distance of $\text{Al}-\text{C}_{\text{SIMes}}$ was significantly longer in comparison with recently reported $(^i\text{Bu})_2\text{Al}(\text{O}, \text{C}_{\text{NHC}})$,^{12h} where $\text{O}, \text{C}_{\text{NHC}}$ represents monoanionic chelate alkoxide ligand with saturated NHC termini.

The ^1H NMR of **1a** in toluene- d_8 and **1b** in THF- d_8 , as well as the corresponding reaction mixtures of $[\text{Me}_2\text{Al}(\mu\text{-OMe})]_3$ and IMes/SIMes ($\text{Al}/\text{NHC} = 1:1$), revealed the instant ligand disproportionation, which was evidenced by the presence of signals corresponding to $\text{Me}_2\text{AlOMe}(\text{NHC})$ and $\text{Me}_3\text{Al}(\text{NHC})$ ($\text{NHC} = \text{IMes}, \text{SIMes}$) complexes (see the Supporting Information). Notably, the ^1H NMR of the reaction mixture of $[\text{Me}_2\text{Al}(\mu\text{-OMe})]_3$ and IMes ($\text{Al}/\text{IMes} = 1:1$) in toluene- d_8 showed essentially a single set of signals, and only traces of decomposition products ($\text{Me}_2\text{AlOMe}(\text{IMes})/\text{Me}_3\text{Al}(\text{NHC}) = 96:4$). However, in all cases discussed above, further decomposition in time was observed (see the Supporting Information). For both **1a** and **1b**, considerably higher-field shifted signals corresponding to $\text{Al}-\text{Me}$ protons (**1a**: – 1.09 ppm, toluene- d_8 , **1b**: – 1.65 ppm, THF- d_8) were in line with the formation of $\text{Al}-\text{C}_{\text{NHC}}$ bonds and $\text{Me}_2\text{AlOMe}(\text{NHC})$ complexes. Although carbene carbon signals in ^{13}C NMR can be indicative for the strength of $\text{M}-\text{C}_{\text{NHC}}$ bonds,²⁰ they could not be observed for both **1a** and **1b**, as well as the corresponding reaction mixtures, even over prolonged acquisition times.

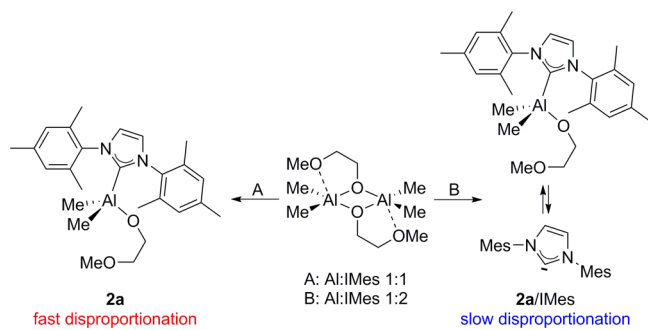
In order to further investigate the structure of $\text{Me}_2\text{AlOR}(\text{NHC})$ complexes, including the strength of $\text{Al}-\text{C}_{\text{NHC}}$ bond, we initially attempted to synthesize $\text{Me}_2\text{Al}(\text{OCH}_2\text{CH}_2\text{OMe})(\text{IMes})$ (**2a**), which formed instantly in the reaction between $[\text{Me}_2\text{Al}(\mu\text{-OCH}_2\text{CH}_2\text{OMe})]_n$ and IMes (Scheme 3, path A, Scheme 4). Contrary to analogous $\text{Me}_2\text{In}(\text{OCH}_2\text{CH}_2\text{OMe})(\text{NHC})$ indium complexes that could be barely observed due to instant and complete disproportionation,⁶ **2a** was dominant in the reaction mixture. Alas, in this case also, ligand disproportionation leading to the complex mixture of products, including $\text{Me}_3\text{Al}(\text{NHC})$ ($\text{NHC} = \text{IMes}, \text{SIMes}$), precluded its isolation. However, colorless crystals of **2a**, suitable for X-ray analysis, were isolated from the reaction mixture of $[\text{Me}_2\text{Al}(\mu\text{-OCH}_2\text{CH}_2\text{OMe})]_n$ and IMes ($\text{Al}/\text{IMes} = 1:2$) – **2a}/\text{IMes} (Scheme 3, path B). The coordination of the IMes ligand to aluminum in **2a** resulted in the formation of complexes with essentially symmetric alignment of IMes ligand, similarly to the analogous dimethylgallium derivative, which is evidenced by $\text{C}(\text{Me})-\text{Al}-\text{C}(1)-\text{N}(1)$ torsion angles (Figure 2). Importantly, the distance and valency of $\text{Al}-\text{C}_{\text{IMes}}$ bond ($2.074(2)$ Å, 0.65 vu - valence units²¹) indicated the similar strength of $\text{Al}-\text{C}_{\text{IMes}}$ in **2a** and $\text{Ga}-\text{C}_{\text{IMes}}$ in $\text{Me}_2\text{Ga}((\text{S})\text{-OCH}(\text{Me})-$**

Table 1. Selected Structural and ^{13}C NMR Data for $\text{Me}_2\text{MOR}(\text{NHC})$ ($\text{M} = \text{Al}, \text{Ga}, \text{In}$; $\text{NHC} = \text{IMes}, \text{SIMes}$)

	N–C–N (deg) ^a	M–C _{NHC} valency (vu) ^c	^{13}C NMR C _{carbene} (ppm)
$\text{Me}_2\text{AlOMe}(\text{IMes})$ (1a)	103.55(12) ($\Delta = 2.1$) ^b	0.64	
$\text{Me}_2\text{GaOMe}(\text{IMes})$ ^{5b}	103.83(9) ($\Delta = 2.4$) ^b	0.65	176.1 ($\Delta = -43.6$) ^c
$\text{Me}_2\text{InOMe}(\text{IMes})$ (SI2)	103.98(15) ($\Delta = 2.6$) ^b	0.65	
$\text{Me}_2\text{AlOMe}(\text{SIMes})$ (1b)	107.9(3) ($\Delta = 3.19$) ^b	0.59	
$\text{Me}_2\text{GaOMe}(\text{SIMes})$ ^{5a}	108.57(12) ($\Delta = 3.9$) ^b	0.63	
$\text{Me}_2\text{InOMe}(\text{SIMes})$ ⁶	108.0(5) ($\Delta = 3.3$) ^b	0.60	
$\text{Me}_2\text{AlOCH}_2\text{CH}_2\text{OMe}(\text{IMes})$ (2a)	103.52(15) ($\Delta = 2.1$) ^b	0.65	174.9 ($\Delta = -44.8$)
$\text{Me}_2\text{GaOCH}_2\text{CH}_2\text{OMe}(\text{IMes})$ (SI1)	104.06(16) ($\Delta = 2.6$)	0.68	176.3 ($\Delta = -43.4$)
$\text{Me}_2\text{AlOCH}_2\text{CH}_2\text{OMe}(\text{SIMes})$			198.2 ($\Delta = -46.2$)
$\text{Me}_2\text{GaOCH}_2\text{CH}_2\text{OMe}(\text{SIMes})$ ^{5b}	108.45(11) ($\Delta = 3.7$)	0.65	200.2 ($\Delta = -44.2$)
$\text{Me}_2\text{Al}(\text{OCPh}_2\text{Me})(\text{IMes})$ (3a)	102.52(17) ($\Delta = 1.1$) ^b	0.64	175.0 ($\Delta = -44.7$)
$\text{Me}_2\text{Ga}(\text{OCPh}_2\text{Me})(\text{IMes})$ ⁶	103.8(3) ($\Delta = 2.4$) ^b	0.64	176.6 ($\Delta = -43.1$) ^c
	103.9(3) ^d ($\Delta = 2.5$) ^b	0.64	
$\text{Me}_2\text{In}(\text{OCPh}_2\text{Me})(\text{IMes})$ ⁶	105.4(7) ($\Delta = 4.0$) ^b	0.61	181.5 ($\Delta = -38.2$) ^c
	104.8(7) ^d ($\Delta = 3.4$) ^b	0.61	
$\text{Me}_2\text{Al}(\text{OCPh}_2\text{Me})(\text{SIMes})$			198.1 ($\Delta = -46.3$)
$\text{Me}_2\text{Ga}(\text{OCPh}_2\text{Me})(\text{SIMes})$ ⁶			199.9 ($\Delta = -44.5$) ^c
$\text{Me}_2\text{In}(\text{OCPh}_2\text{Me})(\text{SIMes})$ ⁶			205.5 ($\Delta = -38.9$) ^c
$\text{Me}_2\text{Al}(\text{OC}_6\text{H}_4\text{OMe})(\text{IMes})$ (4a)	103.52(10) ($\Delta = 2.1$)	0.65	175.5 ($\Delta = -44.2$)
$\text{Me}_2\text{Al}(\text{OC}_6\text{H}_4\text{OMe})(\text{SIMes})$ (4b)			198.6 ($\Delta = -45.8$)
$\text{Me}_2\text{Ga}(\text{OC}_6\text{H}_4\text{OMe})(\text{SIMes})$ ²²			199.2 ($\Delta = -45.2$)

^aRefers to the N(1)–C(1)–N(2) angle. ^bIn comparison with SIMes or IMes. ^cIn comparison with SIMes or IMes in toluene-*d*₈. ^dFor the second independent molecule of the asymmetric unit. ^eBond valence was calculated according to the method described by Brown and Altermatt.²¹

Scheme 3. Reaction of $[\text{Me}_2\text{Al}(\mu\text{-OCH}_2\text{CH}_2\text{OMe})]_2$ with IMes



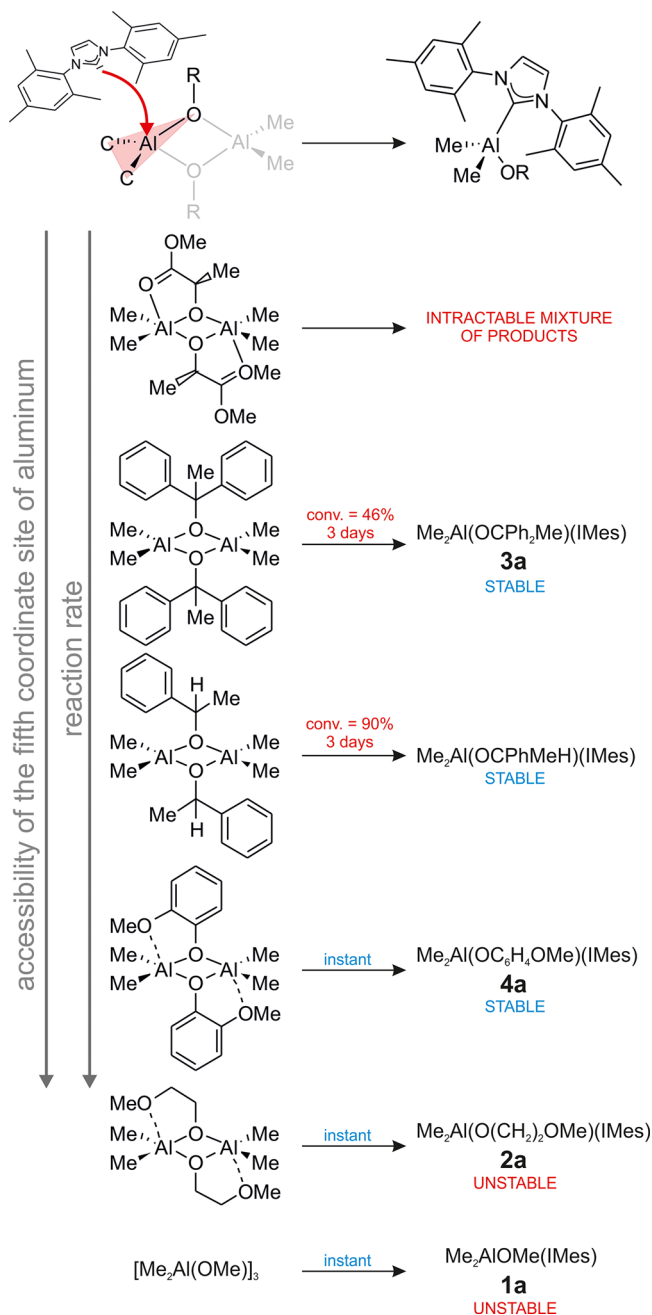
$\text{CH}_2\text{OMe})(\text{IMes})$ ($\text{vu} = 0.64$),^{5b} however slightly weaker in comparison with $\text{Ga}-\text{C}_{\text{IMes}}$ in $\text{Me}_2\text{Ga}(\text{OCH}_2\text{CH}_2\text{OMe})(\text{IMes})$ (**SI1**, $\text{vu} = 0.68$) (Table 1).

While **2a** was unstable in solution, ^1H NMR of **2a**/IMes revealed the presence of a single set of signals corresponding to $\text{Me}_2\text{Al}(\text{OCH}_2\text{CH}_2\text{OMe})(\text{IMes})$ (**2a**) and additional signals corresponding to IMes. In the latter case, the excess of IMes resulted in the stabilization of $\text{Me}_2\text{AlOR}(\text{NHC})$ species, although slow disproportionation was observed in time. Notably, the presence of essentially uncoordinated IMes molecule of **2a**/IMes was evidenced by the carbene carbon signal in ^{13}C NMR (217.3 ppm), considerably shifted to lower field in comparison with the IMes coordinated to aluminum of **2a** (174.9 ppm, $\Delta = -44.8$ ppm). The stability of **2a** in **2a**/IMes could be explained by the interaction of IMes with aluminum of **2a** resulting in the exchange of coordinated/uncoordinated IMes molecules, which was confirmed by ROESY (Rotating frame Overhauser Effect Spectroscopy) experiment (Figure S15). Moreover, in light of the exchange of coordinated/uncoordinated IMes molecule, the shift of uncoordinated IMes by approximately 2 ppm, in comparison with free IMes (219.7

ppm), could be associated with its interaction with aluminum, leading to the stabilization of the $\text{Me}_2\text{Al}(\text{OCH}_2\text{CH}_2\text{OMe})(\text{IMes})$ species. Analogously, the $\text{Me}_2\text{Al}(\text{OCH}_2\text{CH}_2\text{OMe})(\text{SIMes})$ species were more stable in the case of $\text{Me}_2\text{Al}(\text{OCH}_2\text{CH}_2\text{OMe})(\text{SIMes})/\text{SIMes}$ mixture, in comparison with $\text{Me}_2\text{Al}(\text{OCH}_2\text{CH}_2\text{OMe})(\text{SIMes})$, and characterized using NMR spectroscopy (Table 1, see the Supporting Information). Notably, the stabilization of both **2a** and $\text{Me}_2\text{Al}(\text{OCH}_2\text{CH}_2\text{OMe})(\text{SIMes})$, in the case of **2a**/IMes and $\text{Me}_2\text{Al}(\text{OCH}_2\text{CH}_2\text{OMe})(\text{SIMes})/\text{SIMes}$, respectively, was in contrast to the stability of indium $\text{Me}_2\text{InOR}(\text{NHC})$ ($\text{NHC} = \text{IMes}, \text{SIMes}$) species, which revealed the increased tendency for the ligand disproportionation in the presence of excess of NHC.⁶ Interestingly, despite the tendency of $\text{Me}_2\text{Al}(\text{OCH}_2\text{CH}_2\text{OMe})(\text{NHC})$ ($\text{NHC} = \text{IMes}, \text{SIMes}$) to disproportionate, the shift of carbene carbon of IMes/SIMes upon coordination to aluminum, indicated the presence of an $\text{Al}-\text{C}_{\text{NHC}}$ bond of a similar strength to $\text{Ga}-\text{C}_{\text{NHC}}$ in respective stable $\text{Me}_2\text{Ga}(\text{OCH}_2\text{CH}_2\text{OMe})(\text{NHC})$ complexes (Table 1).

With regard to the previously investigated $\text{Me}_2\text{M}(\text{OCH}(\text{Me})\text{CO}_2\text{Me})(\text{NHC})$ complexes, which mimic active species with a growing PLA chain, in the polymerization of lactide with $\text{Me}_2\text{MOR}(\text{NHC})$ ($\text{M} = \text{Ga}, \text{In}$; $\text{NHC} = \text{IMes}, \text{SIMes}$),^{5,6} we approached the synthesis of analogous $\text{Me}_2\text{Al}((S)\text{-OCH}(\text{Me})\text{CO}_2\text{Me})(\text{NHC})$ ($\text{Me}_2\text{Al}((S)\text{-melac})(\text{NHC})$) complexes. However, the reaction of $[\text{Me}_2\text{Al}(\mu\text{-}(S)\text{-melac})]_2$ with IMes or SIMes resulted in oily products with complex ^1H NMR spectra (see the Supporting Information). Interestingly, the presence of several singlets corresponding to $\text{Al}-\text{Me}$ protons suggested in this case the formation of asymmetric dimeric species with coordinated NHC rather than monomeric $\text{Me}_2\text{Al}((S)\text{-melac})(\text{NHC})$ complexes, although the formation of the latter could not be excluded unequivocally. However, the detailed investigation of the structure of resulting complexes, as well as the possibility of the formation of $\text{Me}_2\text{Al}((S)\text{-melac})(\text{NHC})$ in time, was severely limited by the

Scheme 4. Reaction of IMes towards $[\text{Me}_2\text{Al}(\mu\text{-OR})]_n$ ($n = 2,3$) Complexes with Variable Accessibility of the Fifth Coordinate Site of Aluminum (Al/IMes = 1:1) at Room Temperature



ligand disproportionation, which was evidenced by the formation of, among others, $\text{Me}_3\text{Al}(\text{NHC})$ (see the [Supporting Information](#)). While the ligand disproportionation of dialkylaluminum (*S*)-*melac* derivatives upon interaction with NHCs should not be surprising in light of the low stability of $\text{Me}_2\text{AlOR}(\text{NHC})$, the lack of instant formation of $\text{Me}_2\text{Al}((\text{S})\text{-melac})(\text{NHC})$ upon addition of IMes/SIMes to $[\text{Me}_2\text{Al}(\mu\text{-}(\text{S})\text{-melac})]_2$ should be surprising in light of facile synthesis of both stable $\text{Me}_2\text{Ga}((\text{S})\text{-melac})(\text{NHC})$ ^{5a,b} and unstable $\text{Me}_2\text{In}((\text{S})\text{-melac})(\text{NHC})$ ⁶ (NHC = IMes, SIMes) complexes. With regard to the higher stability of $\text{Me}_2\text{AlOR}(\text{NHC})$ in comparison with $\text{Me}_2\text{InOR}(\text{NHC})$ complexes (see above), the instant formation of $\text{Me}_2\text{Al}((\text{S})\text{-melac})(\text{NHC})$ followed by its quick

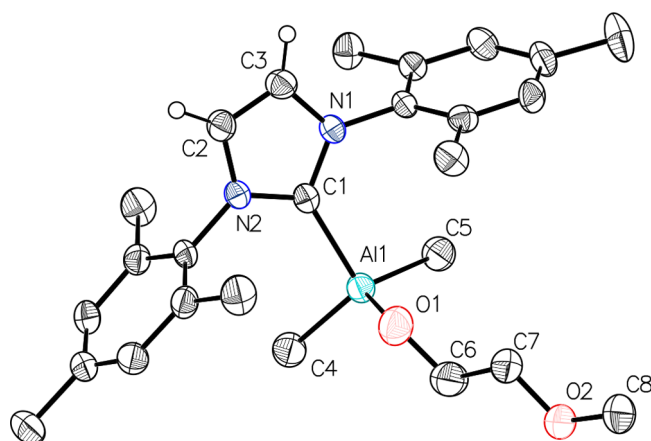


Figure 2. Molecular structure of **2a** with thermal ellipsoids at the 50% probability level. Hydrogen atoms are omitted for clarity. Selected bond lengths (Å) and angles (deg) for **2a**: Al(1)–C(4) 1.977(2), Al(1)–C(5) 1.984(2), Al(1)–C(1) 2.074(2), Al(1)–O(1) 1.756(2), C(1)–Al(1)–C(4) 108.38(8), C(1)–Al(1)–C(5) 109.48(8), C(1)–Al(1)–O(1) 99.68(8), N(1)–C(1)–N(2) 103.52(15), C(5)–Al(1)–C(1)–N(1) 26.44(13), C(4)–Al(1)–C(1)–N(1) 147.48(14), O(1)–Al(1)–C(1)–N(1) 92.02(12), NHC tilt 1.6(1).¹⁷

disproportion does not seem to be likely. On the other hand, limited accessibility of aluminum in $[\text{Me}_2\text{Al}(\mu\text{-}(\text{S})\text{-melac})]_2$ for NHC could promote different reaction pathways, as we have demonstrated for instance for the reactions of $[\text{Me}_2\text{M}(\mu\text{-}(\text{S})\text{-melac})]_2$ ($\text{M} = \text{Ga}, \text{In}$) complexes with bulky NHCs such as SIPr (1,3-bis(2,6-diisopropylphenyl)-imidazolin-2-ylidene)^{5b} or 6-Mes.^{5c} As the smaller ionic radius of aluminum, in comparison with gallium and indium, could be expected to affect the formation of Al–C_{NHC} bonds (see below), it should not limit, to such an extent, the formation of $\text{Me}_2\text{Al}((\text{S})\text{-melac})(\text{NHC})$ given the instant reaction of $[\text{Me}_2\text{Al}(\mu\text{-OCH}_2\text{CH}_2\text{OMe})]_2$ toward IMes/SIMes (Scheme 4). On the contrary, the strongest chelate C=O⋯Al bond, among C=O⋯M of $[\text{Me}_2\text{M}(\mu\text{-}(\text{S})\text{-melac})]_2$ ($\text{M} = \text{Al},^{23} \text{Ga},^{24} \text{In}^{25}$) complexes, could rather be responsible for limited reactivity of $[\text{Me}_2\text{Al}(\mu\text{-}(\text{S})\text{-melac})]_2$ toward SIMes/IMes, and the impaired formation of the Al–C_{NHC} bond of $\text{Me}_2\text{Al}((\text{S})\text{-melac})(\text{NHC})$ complexes. Such a chelate bond of high directionality, typical of five-coordinate dialkylaluminum derivatives, should be expected to severely limit the access of NHC to the CCO face of the tetrahedral coordination sphere of aluminum in $[\text{Me}_2\text{Al}(\mu\text{-OR})]_2$, trans to the Al–O_{bridging} bond (Scheme 4),²⁶ which has already been shown to be crucial for the structure of $[\text{R}_2\text{Al}(\text{O},\text{X})]_n$ ($n = 1,2$; O,X = monoanionic alkoxide/aryloxy ligand with Lewis Base termini),²⁷ reactivity of $[\text{Me}_2\text{Al}(\mu\text{-}(\text{S})\text{-melac})]_2$ in the ROP of cyclic esters,²⁸ and activity of dialkylaluminum alkoxides toward molecular oxygen.²⁹ Similarly, our results on the reactivity of dialkylaluminum alkoxides toward NHCs, discussed below, revealed that the accessibility of the fifth coordinate site of aluminum was the main factor affecting the formation of Al–C_{NHC} and $\text{Me}_2\text{AlOR}(\text{NHC})$ complexes. However, the character of the Al–C_{NHC} bond could also be responsible for the difficulties in breaking of Al_2O_2 bridges and the subsequent formation of $\text{Me}_2\text{Al}((\text{S})\text{-melac})(\text{NHC})$ complexes.

The synthesis of stable $\text{Me}_2\text{AlOR}(\text{NHC})$ and $\text{Me}_2\text{AlOAr}(\text{NHC})$ (OAr = aryloxy group) (NHC = IMes, SIMes) was essential in order to investigate the strength and character of

the Al–C_{NHC} bond using spectroscopic techniques. On the other hand, the careful choice of alkoxide and aryloxy ligands of different steric and electronic properties (Scheme 4) was crucial in order to explain how far the access to the fifth coordinate site is important for the synthesis of dialkylaluminum alkoxides and aryloxides with NHCs. Therefore for the synthesis of Me₂AlOR(NHC) and Me₂AlOAr(NHC) complexes, we chose [Me₂Al(μ-OCPh₂Me)]₂, [Me₂Al(μ-OCPhMeH)]₂, and [Me₂Al(μ-OC₆H₄OMe)]₂ in which bulky alkoxide/aryloxy groups of different steric demands should to a different extent limit the access to the fifth coordinate site of Al in *trans* position to one of Al–O_{bridging} bonds (Scheme 4). Importantly, the reaction of selected dialkylaluminum alkoxides and aryloxides (Figure 3) should lead to the synthesis of

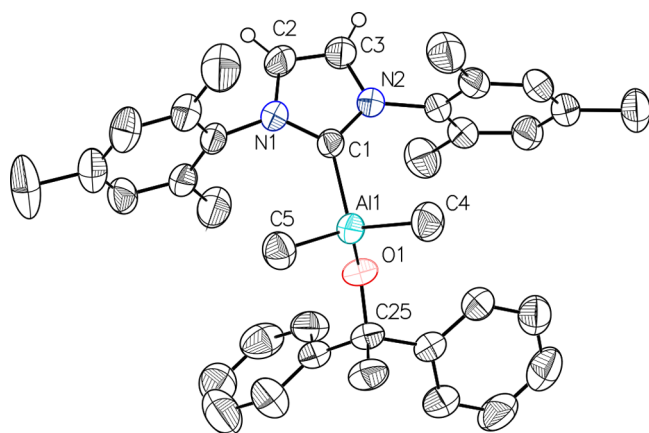


Figure 3. Molecular structure of **3a** with thermal ellipsoids at the 50% probability level. Hydrogen atoms are omitted for clarity. Selected bond lengths (Å) and angles (deg): Al(1)–C(4) 1.976(2), Al(1)–C(5) 1.978(2), Al(1)–C(1) 2.080(2), Al(1)–O(1) 1.750(2), C(1)–Al(1)–C(4) 109.70(9), C(1)–Al(1)–C(5) 107.37(9), C(1)–Al(1)–O(1) 98.09(8), N(1)–C(1)–N(2) 102.52(17), C(5)–Al(1)–C(1)–N(1) 23.13(13), C(4)–Al(1)–C(1)–N(1) 143.63(14), O(1)–Al(1)–C(1)–N(1) 98.08(12), NHC tilt 3.2(1).¹⁷

stable Me₂AlOR(NHC) (OR = OCPh₂Me, OCPhMeH) and Me₂AlOAr(NHC) (OAr = OC₆H₄OMe) complexes, similarly to stable indium complexes - Me₂In(OCPh₂Me)(NHC) (NHC = IMes, SIMes, 6-Mes) recently reported by us, despite the observed tendency of Me₂InOR(NHC) to disproportionate.^{5c,6}

Synthesis and Structure of Me₂AlOR(NHC) (OR = OCPh₂Me, OCPhMeH) Alkoxide Complexes with Bulky Alkoxide Groups. Although initially we did not observe any reaction between NHC (NHC = IMes, SIMes) and [Me₂Al(μ-OCPh₂Me)]₂ (Al/NHC = 1:1), which was evidenced, among others by the presence of essentially free NHC in solution, the slow formation of stable Me₂Al(OCPh₂Me)(NHC) (NHC = IMes (**3a**), SIMes) complexes was observed within days and evidenced by ¹H NMR spectroscopy (see the Supporting Information). The reaction of [Me₂Al(μ-OCPh₂Me)]₂ with IMes led to 97% conversion after 11 days at r.t., which allowed for the isolation of **3a** as colorless crystals in high yield. Although Me₂Al(OCPh₂Me)(SIMes) was also formed in the analogous reaction, much longer reaction times at r.t. were required (85% conversion after 77 days). In order to confirm that limited accessibility of the fifth coordinate site of aluminum in [Me₂Al(μ-OCPh₂Me)]₂ was crucial for its reactivity with NHC, we investigated the synthesis of

Me₂M(OCPhMeH)(IMes) in the reaction of IMes with [Me₂Al(μ-OCPhMeH)]₂ (Scheme 4). The decrease of steric hindrances of the alkoxide ligand in the case of [Me₂Al(μ-OCPhMeH)]₂ resulted in considerably shorter reaction times of the latter with IMes, leading to the formation of stable Me₂Al(OCPhMeH)(IMes) with 90% conversion after 3 days at room temperature (see the Supporting Information). However, the monocrystals suitable for X-ray analysis were obtained only for **3a** (Figure 3). Similarly to previously reported Me₂M(OCPh₂Me)(NHC) (M = Ga, In) complexes, the coordination of IMes ligand to aluminum in **3a** resulted in the formation of asymmetrical complexes, due to the orientation of the IMes ligand respectively to M–C_{Me} bonds, with the aluminum coordination sphere adopting a distorted tetrahedral geometry. In contrast to **1a**, no CH⋯O interactions were observed in the solid state. Instead, CH⋯π interactions and CH⋯HCH₂Al dihydrogen bonds³⁰ could be distinguished. The presence of the strong Al–C_{NHC} bond was mainly supported by the length and valency of Al–C_{NHC} bond (2.080(2) Å, 0.64 vu) (Table 1) and further confirmed by a small NHC tilt (Figure 3). Noteworthy the strength of the Al–C_{IMes} bond in **3a** was comparable to Ga–C_{IMes} (0.64 vu), and considerably stronger than In–C_{IMes} (0.61 vu), in analogous Me₂M(OCPh₂Me)(IMes) (M = Ga, In) complexes,⁶ while the opposite trend was observed for Δ_{NCN} of **3a** (1.1°), Me₂Ga(OCPh₂Me)(IMes) (2.4° and 2.5°) and Me₂In(OCPh₂Me)(IMes) (4.0° and 3.4°) complexes. For **3a** the observed tendency resulted, most probably, from the smallest ionic radii of Al, and therefore the proximity of IMes mesityl rings and Al–Me groups, which precluded the increase in Δ_{NCN} beyond 1.1°, as it would require pushing mesityl rings even further toward Al–Me groups (Figure 3). Interestingly, the latter did not affect the strength of the Al–C_{IMes} bond, which was comparable to **1a** and **2a**. It also did not cause noticeable constraints within the coordination sphere of aluminum, which was evidenced by the short resultant bond valence vector (BVV)³¹ of 0.049 vu (Figure S58).³² It must therefore be noted that Δ_{NCN} is sensitive to steric hindrances, especially in the presence of sterically bulky ligands, and as such should not be considered as a precise measure of M–C_{NHC} bond strength.²⁰

The ¹H NMR of both **3a** and Me₂Al(OCPh₂Me)(SIMes) in toluene-*d*₈ revealed a single set of signals with Al–Me protons at –1.23 ppm and –1.31 ppm, respectively, shifted to considerably higher-field in comparison with [Me₂Al(μ-OCPh₂Me)]₂. Importantly, in contrast to **1** and **2**, both **3a** and Me₂Al(OCPh₂Me)(SIMes) were stable in solution over weeks. The ¹³C NMR carbene carbon shift of **3a**, and the difference between the latter and free IMes, are indicative of a strong Al–C_{IMes} bond (175.0 ppm, Δ = –44.7 ppm), slightly stronger than Ga–C_{NHC} (176.6 ppm, Δ = –43.1 ppm), and significantly stronger in comparison with the In–C_{NHC} bond (181.5 ppm, Δ = –38.2 ppm) of Me₂M(OCPh₂Me)(NHC) (M = Ga, In) (Table 1). Similarly to the latter, the largest shift of the carbene carbon among Me₂M(OCPh₂Me)(SIMes) (M = Al (198.1 ppm, Δ = –46.3 ppm), Ga (199.9 ppm, Δ = –44.5 ppm),⁶ and In (205.5 ppm, Δ = –38.9 ppm)⁶ complexes was observed for the aluminum derivative, indicating the strongest Al–C_{NHC} bond among M–C_{NHC} bonds of Me₂M(OCPh₂Me)(NHC) (M = Al, Ga, In; NHC = IMes, SIMes) complexes. Although we have recently shown that the shift of the carbene carbon should not be considered a precise measure of the strength of M–C_{NHC} bonds,^{5c} it should be noted that the

strength of $M-C_{\text{NHC}}$ bond of $\text{Me}_2\text{M}(\text{OCPh}_2\text{Me})(\text{NHC})$ ($M = \text{Al}, \text{Ga}, \text{In}$; $\text{NHC} = \text{IMes}, \text{SIMes}$) complexes in solution, estimated on the basis of ^{13}C NMR spectroscopy, i.e., $\text{Al}-C_{\text{NHC}} > \text{Ga}-C_{\text{NHC}} \gg \text{In}-C_{\text{NHC}}$, is essentially in line with $\text{Al}-C_{\text{NHC}} \approx \text{Ga}-C_{\text{NHC}} > \text{In}-C_{\text{NHC}}$ determined on the basis of $M-C_{\text{IMes}}$ bond lengths (and valency) in the solid state (Table 1). The examples above not only showed that stable $\text{Me}_2\text{AlOR}(\text{NHC})$ with bulky alkoxide ligands can be synthesized similarly to their stable gallium and indium analogues.⁶ They also confirmed that the directionality of the effective interaction of the NHC to the fifth coordinate site of dimeric $[\text{Me}_2\text{Al}(\mu\text{-OR})_2]$ is crucial for the coordination of NHC to aluminum, the subsequent breaking of Al_2O_2 bridges, and finally the formation of monomeric $\text{Me}_2\text{AlOR}(\text{NHC})$ complexes.

Synthesis and Structure of $\text{Me}_2\text{AlOAr}(\text{NHC})$ Aryloxy Complexes. The reaction between NHC ($\text{NHC} = \text{IMes}, \text{SIMes}$) and $[\text{Me}_2\text{Al}(\mu\text{-OC}_6\text{H}_4\text{OMe})_2]$ ($\text{Al}/\text{NHC} = 1:1$) at room temperature led to the instant formation of $\text{Me}_2\text{Al}(\text{OC}_6\text{H}_4\text{OMe})(\text{NHC})$ ($\text{NHC} = \text{IMes}$ (**4a**) and SIMes (**4b**)). Instant reaction of $[\text{Me}_2\text{Al}(\mu\text{-OC}_6\text{H}_4\text{OMe})_2]$ and NHC ($\text{NHC} = \text{IMes}$ or SIMes) should be interpreted in terms of much higher availability of CCO face of tetrahedral coordination sphere of aluminum in $[\text{Me}_2\text{Al}(\mu\text{-OC}_6\text{H}_4\text{OMe})_2]$ in comparison with $[\text{Me}_2\text{Al}(\mu\text{-OCPh}_2\text{Me})_2]$ and $[\text{Me}_2\text{Al}(\mu\text{-OCPhMeH})_2]$ (Scheme 4), which should be due to the presence of weak chelate bond between aluminum and methoxide group of 2-methoxyphenol, similarly to $[\text{Me}_2\text{Al}(\mu\text{-OCH}_2\text{CH}_2\text{OMe})_2]$ (see above). Moreover, significantly weaker Al_2O_2 bridges in the case of dialkylaluminum aryloxides should facilitate the formation of $\text{Me}_2\text{Al}(\text{OC}_6\text{H}_4\text{OMe})(\text{NHC})$. **4a** and **4b** were isolated as colorless crystals in high yields. However, crystals suitable for X-ray analysis could only be obtained in the case of **4a**. The X-ray analysis of **4a** revealed the presence of a monomeric aluminum complex with the coordination sphere of aluminum adopting a distorted tetrahedral geometry. The orientation of the IMes ligand was asymmetric with respect to $\text{Al}-C_{\text{Me}}$ bonds, which was reflected by $\text{C}(\text{Me})-\text{Al}-C_{\text{NHC}}-\text{N}$ torsion angles (Figure 4). As a result, the ipso carbon of the mesityl group of IMes was located, similarly to **1a**, essentially

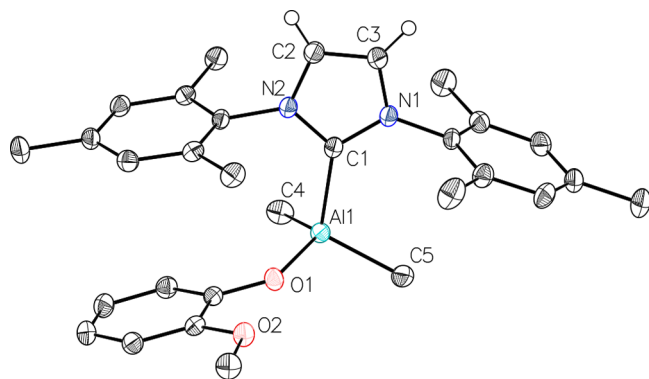


Figure 4. Molecular structure of **4a** with thermal ellipsoids at the 30% probability level. Hydrogen atoms are omitted for clarity. Selected bond lengths (Å) and angles (deg): $\text{Al}(1)-\text{C}(4)$ 1.978(1), $\text{Al}(1)-\text{C}(5)$ 1.971(1), $\text{Al}(1)-\text{C}(1)$ 2.073(1), $\text{Al}(1)-\text{O}(1)$ 1.764(1), $\text{C}(1)-\text{Al}(1)-\text{C}(4)$ 107.23(5), $\text{C}(1)-\text{Al}(1)-\text{C}(5)$ 109.87(5), $\text{C}(1)-\text{Al}(1)-\text{O}(1)$ 104.39(5), $\text{N}(1)-\text{C}(1)-\text{N}(2)$ 103.52(10), $\text{C}(5)-\text{Al}(1)-\text{C}(1)-\text{N}(1)$ 12.71(10), $\text{C}(4)-\text{Al}(1)-\text{C}(1)-\text{N}(1)$ 108.74(10), $\text{O}(1)-\text{Al}(1)-\text{C}(1)-\text{N}(1)$ 128.16(9), NHC tilt 3.6(1).¹⁷

over one of the methyl groups, while the phenyl ring of 2-methoxyphenol faced the other mesityl group of IMes, which likely resulted from the π -stacking of the aromatic rings. Alternatively, it could be also caused by the $(\text{mesityl})_2\text{CH}\cdots\text{O}_{\text{aryloxyde}}$ and $(\text{IMes central ring})\text{CH}\cdots\text{OMe}$ weak interactions, leading to the chain structure of **4a** in a solid state (see the Supporting Information). Interestingly, the orientation of $\text{OC}_6\text{H}_4\text{OMe}$ precluded in this case the interaction of OMe group to the fifth coordinate site of aluminum. The lack of $\text{Al}\cdots\text{OMe}$ chelate interaction in the solid state could also be rationalized by the presence of strong $\text{Al}-C_{\text{NHC}}$. Importantly, the strength of $\text{Al}-C_{\text{NHC}}$ of **4a** in the solid state was evidenced mainly by the distance and bond valence of $\text{Al}-C_{\text{IMes}}$ bond (2.0733(13) Å, 0.65 vu). However, as a result of the smaller steric hindrance of the aryloxyde ligand, in comparison with the OCPh_2Me alkoxide ligand, we observed a more significant increase of the NCN angles of **4a** ($103.52(10)^\circ$, $\Delta = 2.1^\circ$), in comparison with free IMes¹⁸ and SIMes,¹⁹ much larger than in the case **3a** ($102.52(17)^\circ$, $\Delta = 1.1^\circ$) and similar to methoxide derivative **1a** ($103.55(12)^\circ$, $\Delta = 2.1^\circ$).

In solution, complexes **4a** and **4b** showed no tendency for ligand disproportionation similarly to analogous $\text{Me}_2\text{In}(\text{OC}_6\text{H}_4\text{OMe})(\text{NHC})$ aryloxides.^{5c} The ^{13}C NMR carbene carbon shifts, as well as the differences between free and coordinated NHC, were indicative in the case of **4a** (176.4 ppm, $\Delta = -43.3$ ppm) and **4b** (198.6 ppm, $\Delta = -45.8$ ppm) of the strength of $\text{Al}-C_{\text{NHC}}$ bonds (Table 1). They revealed the similar strength of $\text{Al}-C_{\text{NHC}}$ and $\text{Ga}-C_{\text{NHC}}$ bonds of $\text{Me}_2\text{Ga}(\text{OC}_6\text{H}_4\text{OMe})(\text{NHC})$ ($\text{NHC} = \text{IMes}$ - 176.0 ppm, $\Delta = -43.7$ ppm; SIMes - 199.2 ppm, $\Delta = -45.2$ ppm) as well as significantly stronger $\text{Al}-C_{\text{NHC}}$ bonds in comparison with the $\text{In}-C_{\text{NHC}}$ bonds of $\text{Me}_2\text{In}(\text{OC}_6\text{H}_4\text{OMe})(\text{NHC})$ ($\text{NHC} = \text{IMes}$ - 183.3 ppm, $\Delta = -34.0$ ppm; SIMes - 206.7 ppm, $\Delta = -37.3$ ppm).²⁰ The formation of stable $\text{Me}_2\text{M}(\text{OC}_6\text{H}_4\text{OMe})(\text{NHC})$ as well as $\text{Me}_2\text{Al}(\text{OCPh}_2\text{Me})(\text{NHC})$ complexes is not surprising in the light of high stability of analogous gallium and indium complexes. However, given the relatively strong $\text{Al}-C_{\text{NHC}}$ bond, evidenced for both $\text{Me}_2\text{AlOAr}(\text{NHC})$ and $\text{Me}_2\text{AlOR}(\text{NHC})$, the tendency of the latter to disproportionate was in opposition to our earlier conclusion on the effect of the strength of $M-C_{\text{NHC}}$ bond ($M = \text{Ga}, \text{In}$) on the stability of $\text{Me}_2\text{MOR}(\text{NHC})$ ($M = \text{Ga}, \text{In}$) complexes.⁶ Although in our previous studies we anticipated that much weaker $\text{In}-C_{\text{NHC}}$ in comparison with $\text{Ga}-C_{\text{NHC}}$ should be responsible for the tendency of dialkylindium complexes with NHC to disproportionate, the above observations concerning the strength of $\text{Al}-C_{\text{NHC}}$ bonds indicated that increased ionic character of $M-C_{\text{NHC}}$ bonds, rather than only their strength, should be responsible for the reactivity of $\text{Me}_2\text{M}(\text{OCPh}_2\text{Me})(\text{NHC})$ ($M = \text{Al}, \text{Ga}, \text{In}$) complexes (see below). Therefore, the stability of these complexes should also be affected by the ionic/covalent character of $M-C_{\text{NHC}}$ bonds.

Ring Opening Polymerization (ROP) of *rac*-LA with $\text{Me}_2\text{AlOR}(\text{NHC})$ and $\text{Me}_2\text{AlOAr}(\text{NHC})$ Complexes. With regard to the catalytic activity of $\text{Me}_2\text{AlOR}(\text{NHC})$ complexes in the ROP of lactide, it must be noted that $\text{Me}_2\text{AlOR}(\text{NHC})$ ($\text{OR} = \text{OMe}, \text{OCH}_2\text{CH}_2\text{OMe}, (\text{NHC} = \text{IMes}, \text{SIMes})$), as well as $\text{Me}_2\text{Al}(\text{OCH}(\text{Me})\text{CO}_2)(\text{NHC})$ which mimic aluminum catalytic species formed by the insertion of *rac*-LA into $\text{Al}-\text{O}_{\text{alkoxide}}$ bond of $\text{Me}_2\text{AlOR}(\text{NHC})$, disproportionate readily. Moreover, according to the literature, the resulting free NHC catalyzes a polymerization of lactide under investigated conditions (see below).³³ Therefore, out of unstable

dimethylaluminumalkoxides discussed above, we investigated only the catalytic activity of $\text{Me}_2\text{AlOMe}(\text{IMes})$ (**1a**) (as the reaction mixture of $[\text{Me}_2\text{Al}(\mu\text{-OMe})_3]$ and IMes/SIMes ; $\text{Al}/\text{NHC} = 1:1$), for which only traces of decomposition products were evidenced (Figure S1). However, in the light of the catalytic activity of $\text{Me}_3\text{Al}(\text{NHC})$,⁹ as well as $\text{Me}_2\text{InOR}(\text{NHC})$,⁶ which allowed for the initiation of *rac*-LA polymerization by NHC, it was interesting to investigate the effect of the character of the $\text{Al}-\text{C}_{\text{NHC}}$ bond on the catalytic properties of stable $\text{Me}_2\text{Al}(\text{OCPh}_2\text{Me})(\text{IMes})$ (**3a**), $\text{Me}_2\text{Al}(\text{OC}_6\text{H}_4\text{OMe})(\text{IMes})$ (**4a**), and $\text{Me}_2\text{Al}(\text{OC}_6\text{H}_4\text{OMe})(\text{SIMes})$ (**4b**).

The polymerization of *rac*-LA with $\text{Me}_2\text{AlOMe}(\text{IMes})$ (**1a**), **3a**, **4a**, and **4b** was performed at -20°C similarly to previously investigated $\text{Me}_2\text{MOR}(\text{NHC})$ ($\text{M} = \text{Ga}, \text{In}$) complexes.^{5,6} Notably, under these conditions, the insertion of *rac*-LA into $\text{In}-\text{C}_{\text{NHC}}$ of $\text{Me}_2\text{InOR}(\text{NHC})$ was observed,^{5c,6} while the significantly stronger $\text{Ga}-\text{C}_{\text{NHC}}$ bond in $\text{Me}_2\text{GaOR}(\text{NHC})$ remained intact.⁵ For the discussed dimethylaluminum alkoxide complexes with IMes , **3a** showed essentially no activity in the polymerization of *rac*-LA at -20°C , even after 24 h, in contrast to $\text{Me}_2\text{In}(\text{OCPh}_2\text{Me})(\text{IMes})$, which polymerized *rac*-LA due to insertion of the latter into the $\text{In}-\text{C}_{\text{IMes}}$ bond. On the other hand analogous $\text{Me}_2\text{Ga}(\text{OCPh}_2\text{Me})(\text{IMes})$ did not reveal any reactivity toward *rac*-LA under the same conditions. However, the observed lack of activity of **3a** should be associated with the steric hindrances of the bulky alkoxide group, limiting the effective interaction of lactide with **3a**, rather than low reactivity of the $\text{Al}-\text{C}_{\text{IMes}}$ bond, in the light of the much more ionic character of the $\text{Al}-\text{C}_{\text{NHC}}$ bond in comparison with $\text{Ga}-\text{C}_{\text{NHC}}$ and $\text{In}-\text{C}_{\text{NHC}}$ bonds and the reactivity of $\text{Me}_2\text{M}(\text{OC}_6\text{H}_4\text{OMe})(\text{NHC})$ ($\text{M} = \text{Al}, \text{Ga}$) (see below). Noteworthy, steric congestion around aluminum center can be crucial for the reactivity of $\text{Al}-\text{NHC}$ motif, which has been also recently observed by Camp and co-workers for aluminum alkoxides and aryloxides stabilized with NHCs.^{12h} Moreover, the activity of $\text{Me}_3\text{Al}(\text{NHC})$ is strongly dependent on the steric hindrances in the Al coordination sphere, in this case on bulkiness of NHC ligand.⁹ Such reasoning was supported by the catalytic activity of **4a** and **4b**, as well as $\text{Me}_2\text{AlOMe}(\text{IMes})$ (**1a**), which polymerized *rac*-LA already at -20°C . In all cases, the resulting PLA was dominantly isotactic ($P_m = 0.76\text{--}0.80$). However, the average molecular weight ($M_n \approx 100\,000$ Da), obtained by gel permeation chromatography (see the Supporting Information), was much higher than expected from a *rac*-LA/Al ratio of 50, indicating that only small fraction of aluminum centers initiated the polymerization of *rac*-LA. Additionally a broad molecular weight distribution was indicative of the uncontrolled nature of the polymerization. MALDI-TOF analyses of high molecular weight PLA, obtained with $\text{Me}_2\text{AlOMe}(\text{IMes})$ (**1a**), **4a**, and **4b**, did not allow for the determination of end groups. Moreover, no insertion of *rac*-LA into $\text{Al}-\text{OC}_6\text{H}_4\text{OMe}$ or $\text{Al}-\text{OMe}$ bonds, leading to PLA with OH and OR end groups, could be evidenced by ^1H NMR spectroscopy. All the above strongly suggested the insertion of *rac*-LA into the $\text{Al}-\text{C}_{\text{NHC}}$ bond, similarly to $\text{Me}_3\text{Al}(\text{NHC})$.⁹ Although in the case of $\text{Me}_2\text{AlOMe}(\text{IMes})$ (**1a**) initiation by free NHC resulting from its disproportionation should also be considered, the insertion of LA exclusively into the $\text{Al}-\text{C}_{\text{NHC}}$ bond should be expected for stable **4a** and **4b** complexes. Interestingly, both a relatively strong $\text{Al}-\text{C}_{\text{NHC}}$ bond in **4a** and **4b**, as well as a weak $\text{In}-\text{C}_{\text{NHC}}$ bond,⁶ in comparison with inert $\text{Ga}-\text{C}_{\text{NHC}}$ bonds in

the analogous $\text{Me}_2\text{Ga}(\text{OC}_6\text{H}_4\text{OMe})(\text{SIMes})$ complex, initiated the ROP of *rac*-LA. Therefore, the reactivity of the $\text{M}-\text{C}_{\text{NHC}}$ bond in the ROP of lactide should be expected to result from the ionic character of $\text{M}-\text{C}_{\text{NHC}}$ bonds, rather than simply their strength. With regard to the effect of $\text{M}-\text{C}_{\text{NHC}}$ bonds on the structure and reactivity of $\text{Me}_2\text{MOR}(\text{NHC})$ ($\text{M} = \text{Al}, \text{Ga}, \text{In}$; $\text{NHC} = \text{IMes}, \text{SIMes}$) complexes, we decided to investigate both the strength and character of $\text{M}-\text{C}_{\text{NHC}}$ bonds using DFT methods.

Computational Studies of Bond Dissociation Energies (BDEs) of $\text{M}-\text{C}_{\text{NHC}}$ Bonds. Bond dissociation energies (BDEs) of the $\text{M}-\text{C}_{\text{NHC}}$ ($\text{M} = \text{Al}, \text{Ga}, \text{In}$; $\text{NHC} = \text{IMes}, \text{SIMes}$) bonds were estimated, using the same approach as in our previous work,^{5b} by calculating the energy of systems **1a**, **1b**, **2a**, and **3a**, as well as analogous gallium and indium complexes, and subtracting the sum of the energies of NHC and aluminum/gallium/indium parts (with the counterpoise correction) (Table 2). In the case of $\text{Me}_2\text{MOMe}(\text{NHC})$ ($\text{M} =$

Table 2. (BDEs) of $\text{M}-\text{C}_{\text{NHC}}$ Bonds of $\text{Me}_2\text{MOR}(\text{NHC})$ ($\text{M} = \text{Al}, \text{Ga}, \text{In}$; $\text{NHC} = \text{IMes}, \text{SIMes}$) Complexes

	BDE (kcal/mol) DFT	BDE (kcal/mol) DLPNO-CCSD(T)
$\text{Me}_2\text{AlOMe}(\text{IMes})$ (1a)	44.4	45.6
$\text{Me}_2\text{GaOMe}(\text{IMes})$	39.6 ^{5b}	40.7
$\text{Me}_2\text{InOMe}(\text{IMes})$ (SI2)	42.2	43.5
$\text{Me}_2\text{AlOMe}(\text{SIMes})$ (1b)	42.5	41.6
$\text{Me}_2\text{GaOMe}(\text{SIMes})$	38.7 ^{5b}	38.9
$\text{Me}_2\text{InOMe}(\text{SIMes})$	41.7	42.1
$\text{Me}_2\text{AlOCH}_2\text{CH}_2\text{OMe}(\text{IMes})$ (2a)	46.2	45.1
$\text{Me}_2\text{GaOCH}_2\text{CH}_2\text{OMe}(\text{IMes})$ (SI1)	42.5	42.3
$\text{Me}_2\text{Al}(\text{OCPh}_2\text{Me})(\text{IMes})$ (3a)	50.0	48.7
$\text{Me}_2\text{Ga}(\text{OCPh}_2\text{Me})(\text{IMes})$	46.1	45.8
$\text{Me}_2\text{In}(\text{OCPh}_2\text{Me})(\text{IMes})$	45.8	44.2

$\text{Al}, \text{Ga}, \text{In}$; $\text{NHC} = \text{IMes}, \text{SIMes}$) complexes, BDEs of $\text{M}-\text{C}_{\text{IMes}}$ bonds are higher in comparison with corresponding $\text{M}-\text{C}_{\text{SIMes}}$ bonds, which is in full agreement with the bond strength obtained from X-ray data (Table 1). On the other hand, calculated BDEs indicate that the strength of $\text{M}-\text{C}_{\text{NHC}}$ bonds increases in series: $\text{Ga}-\text{C}_{\text{NHC}} < \text{In}-\text{C}_{\text{NHC}} < \text{Al}-\text{C}_{\text{NHC}}$, which is in sharp contrast to the strength of $\text{M}-\text{C}_{\text{IMes}}$ and $\text{M}-\text{C}_{\text{SIMes}}$ bonds, determined by X-ray analysis (Table 1). Although, in the case of $\text{Me}_2\text{M}(\text{OCPh}_2\text{Me})(\text{IMes})$ ($\text{M} = \text{Al}, \text{Ga}, \text{In}$), calculated BDEs revealed slightly stronger $\text{Ga}-\text{C}_{\text{IMes}}$ bonds in comparison with $\text{In}-\text{C}_{\text{IMes}}$, the strength of $\text{M}-\text{C}_{\text{IMes}}$ bonds increasing in a row, $\text{In}-\text{C}_{\text{IMes}} < \text{Ga}-\text{C}_{\text{IMes}} < \text{Al}-\text{C}_{\text{IMes}}$, is also not in line with bond valencies calculated on the basis of $\text{M}-\text{C}_{\text{IMes}}$ bond distances ($\text{Al}-\text{C}_{\text{IMes}} \approx \text{Ga}-\text{C}_{\text{IMes}} > \text{In}-\text{C}_{\text{IMes}}$). Finally, the highest BDEs of $\text{Al}-\text{C}_{\text{NHC}}$ bonds, among all investigated $\text{Me}_2\text{MOR}(\text{NHC})$ complexes (Table 2) explain neither the stability nor the reactivity of $\text{Me}_2\text{AlOR}(\text{NHC})$ complexes in comparison with their gallium and indium analogues, which rather depends on the ionic/covalent character of $\text{M}-\text{C}_{\text{NHC}}$ bonds (see below).

Probing the Character of $\text{M}-\text{C}_{\text{NHC}}$ Bonds in $\text{Me}_2\text{MOR}(\text{NHC})$ Using AIM and ELI-D Analysis. Although in our previous studies we suggested that the strength of $\text{M}-\text{C}_{\text{NHC}}$ bonds was decisive for the synthesis, structure, and reactivity of $\text{Me}_2\text{MOR}(\text{NHC})$ ($\text{M} = \text{Ga}, \text{In}$) complexes,⁵ the detailed

Table 3. Calculated Bond Topological^a and Integrated^b Bond Descriptors for M–C_{NHC} of Selected Me₂MOR(NHC) and Me₂MOAr(NHC)^c

	bond	<i>d</i>	ρ_{bcp}	$\nabla^2\rho_{\text{bcp}}$	ϵ	G/ρ_{bcp}	H/ρ_{bcp}	
Me ₂ AlOMe(IMes) (1a)	Al–C _{NHC}	2.082	0.41	5.3	0.05	1.13	–0.23	
Me ₂ GaOMe(IMes)	Ga–C _{NHC}	2.089	0.58	4.1	0.04	0.90	–0.41	
Me ₂ InOMe(IMes)	In–C _{NHC}	2.278	0.50	4.5	0.03	0.90	–0.27	
Me ₂ AlOMe(SIMes) (1b)	Al–C _{NHC}	2.110	0.39	4.8	0.03	1.08	–0.23	
Me ₂ GaOMe(SIMes)	Ga–C _{NHC}	2.101	0.58	3.9	0.04	0.88	–0.41	
Me ₂ InOMe(SIMes)	In–C _{NHC}	2.301	0.48	4.2	0.03	0.87	–0.26	
Me ₂ Al(OCPh ₂ Me)(IMes) (3a)	Al–C _{NHC}	2.080	0.41	5.2	0.01	1.12	–0.23	
Me ₂ Ga(OCPh ₂ Me)(IMes)	Ga–C _{NHC}	2.096	0.58	4.0	0.03	0.89	–0.41	
Me ₂ Ga(OCPh ₂ Me)(6-Mes)	Ga–C _{NHC}	2.139	0.55	3.2	0.01	0.83	–0.41	
Me ₂ In(OCPh ₂ Me)(IMes)	In–C _{NHC}	2.301	0.48	4.2	0.03	0.87	–0.26	
Me ₂ In(OCPh ₂ Me)(6-Mes)	In–C _{NHC}	2.331	0.47	3.8	0.06	0.83	–0.26	
Me ₂ Al(OC ₆ H ₄ OMe)(IMes) (4a)	Al–C _{NHC}	2.073	0.42	5.3	0.04	1.12	–0.24	
Me ₂ Ga(OC ₆ H ₄ OMe)(IMes)	Ga–C _{NHC}	2.072	0.60	4.3	0.09	0.91	–0.41	
Me ₂ In(OC ₆ H ₄ OMe)(IMes)	In–C _{NHC}	2.292	0.49	4.3	0.01	0.88	–0.26	
	basin	δ	V_{001}^{ELI}	ELI _{pop}	ELI _{max}	Δ_{ELI}	RJI (e)	RJI (%)
Me ₂ AlOMe(IMes) (1a)	Al–C _{NHC}	0.20	11.11	2.54	2.32	0.028	2.41(0.09 ^d)	95.0(3.7 ^d)
Me ₂ GaOMe(IMes)	Ga–C _{NHC}	0.46	10.64	2.57	2.08	0.057	2.25	87.5
Me ₂ InOMe(IMes)	In–C _{NHC}	0.48	11.21	2.48	2.06	0.053	2.24	90.3
Me ₂ AlOMe(SIMes) (1b)	Al–C _{NHC}	0.20	9.75	2.34	2.43	0.046	2.21(0.09 ^d)	94.8(4.0 ^d)
Me ₂ GaOMe(SIMes)	Ga–C _{NHC}	0.46	9.24	2.38	2.16	0.070	2.05	86.4
Me ₂ InOMe(SIMes)	In–C _{NHC}	0.47	9.81	2.28	2.14	0.064	2.05	89.8
Me ₂ Al(OCPh ₂ Me)(IMes) (3a)	Al–C _{NHC}	0.20	11.22	2.54	2.34	0.008	2.42(0.09 ^d)	95.0(3.7 ^d)
Me ₂ Ga(OCPh ₂ Me)(IMes)	Ga–C _{NHC}	0.46	10.28	2.55	2.10	0.132	2.24	87.5
Me ₂ Ga(OCPh ₂ Me)(6-Mes)	Ga–C _{NHC}	0.45	8.99	2.35	2.19	0.057	2.02	85.7(13.0)
Me ₂ In(OCPh ₂ Me)(IMes)	In–C _{NHC}	0.47	10.85	2.44	2.09	0.149	2.20	90.3
Me ₂ In(OCPh ₂ Me)(6-Mes)	In–C _{NHC}	0.47	9.94	2.29	2.14	0.026	2.04	89.3(9.1)
Me ₂ Al(OC ₆ H ₄ OMe)(IMes) (4a)	Al–C _{NHC}	0.21	11.27	2.55	2.32	0.042	2.42(0.97 ^d)	94.9(3.8 ^d)
Me ₂ Ga(OC ₆ H ₄ OMe)(IMes)	Ga–C _{NHC}	0.49	10.91	2.60	2.06	0.087	2.25	86.5
Me ₂ In(OC ₆ H ₄ OMe)(IMes)	In–C _{NHC}	0.46	11.11	2.48	2.08	0.146	2.25	90.7

^aDefinitions and units: Bond lengths (*d*) in Å and bond topological properties: electron density ρ_{bcp} in e·Å^{–3} and its corresponding Laplacian $\nabla^2\rho_{\text{bcp}}$ in e·Å^{–5}; ϵ , bond ellipticity; G/ρ_{bcp} and H/ρ_{bcp} , kinetic and total energy density over ρ_{bcp} ratios in he^{-1} . ^bDefinitions and units: δ – the delocalization index; V_{001}^{ELI} , volume of the ELI-D basin in Å³ cut at 0.001 au; ELI_{pop}, electron population within the ELI-D basin in e, ELI_{max}, ELI-D value at the attractor position; Δ_{ELI} , the distance in Å of the attractor position perpendicular to the atom–atom axis; RJI, Raub–Jansen index in e and %. ^cM = Al, Ga, In; NHC = IMes, SIMes, and 6-Mes. ^dRaub–Jansen index value for contribution of aluminum atom.

analysis of Me₂MOR(NHC) (M = Al, Ga, In) complexes (see above) indicated that in addition to the strength of M–C_{NHC} bonds their character should also be considered. In order to estimate the character of M–C_{NHC} bonds in the investigated complexes, we used real-space bonding indicators (RSBIs) obtained from density functional theory (DFT) calculations and topological analysis of the computed electron and pair densities according to the atoms-in-molecules (AIM)³⁴ and electron localizability indicator (ELI-D)³⁵ space partitioning schemes, respectively, which provide a set of topological and integrated bonding and atomic properties. RSBIs have been recently discussed with regard to the determination of the character of interactions between main group elements,³⁶ as well as used for the determination of the character of M–C bonds, including Zn–C³⁷ and Te–C_{NHC}³⁸ bonds. In our studies, we used RSBIs to explain the effect of the character of M–C_{NHC} bonds in Me₂MOR(NHC) (M = Al, Ga, In, NHC = IMes, SIMes) complexes on their synthesis, structure, and reactivity. Additionally, for a more thorough understanding of the character of M–C_{NHC} bonds, we calculated RSBIs for Me₂MOR(6-Mes) (M = Ga, In) complexes recently reported by us, in which weaker M–C_{6-Mes} bonds, in comparison with M–C_{IMes} and M–C_{SIMes} bonds, are present.^{5c}

Starting from the experimental coordinates, gas-phase structures of Me₂MOR(NHC) (M = Al, Ga, In; NHC = IMes, SIMes) complexes such as Me₂MOMe(IMes), Me₂MOMe(SIMes), Me₂M(OCPh₂Me)(IMes), and Me₂M(OC₆H₄OMe)(IMes),³⁹ as well as Me₂M(OCPh₂Me)(6-Mes) (M = Ga, In), were obtained by single-point calculations at the B3PW91/6-311+G(2df,p) level of theory in order to reveal the effect of metal and NHC on the character of M–C_{NHC} bonds. For the investigated complexes, a set of topological and integrated real-space bonding indicators (RSBI) derived from the electron and electron pair densities was calculated and collected in Table 3 (see also the Supporting Information for details). For all M–C_{NHC} bonds, positive values of the corresponding Laplacian $\nabla^2\rho_{\text{bcp}}$ were indicative of strongly polar bonds with dominant ionic contribution. However, the electron densities ρ_{bcp} at the M–C_{NHC} bond critical points ranged from 0.39–0.42 e·Å^{–3} (Al–C_{NHC}), 0.48–0.50 e·Å^{–3} (In–C_{NHC}) and 0.58–0.60 e·Å^{–3} (Ga–C_{NHC}), which indicated the decrease of ionic contribution in a row Al–C_{NHC} > In–C_{NHC} > Ga–C_{NHC} bonds. The delocalization index values confirmed the higher covalent contribution for Ga–C_{NHC} and In–C_{NHC} bonds (for both from 0.46 to 0.49) compared to Al–C_{NHC} ($\delta = 0.2$). Additionally, the kinetic energy density over ρ_{bcp} ratios G/ρ_{bcp} , showing the degree of ionicity, and

especially the total energy density over ρ_{bcp} ratios H/ρ_{bcp} , showing the degree of covalency, indicated the significantly higher (polar) covalent character of Ga–C_{NHC} bonds ($G/\rho_{\text{bcp}} = 0.88\text{--}0.91 \text{ he}^{-1}$, $H/\rho_{\text{bcp}} = -0.41 \text{ he}^{-1}$) in comparison with In–C_{NHC} ($G/\rho_{\text{bcp}} = 0.87\text{--}0.9 \text{ he}^{-1}$, $H/\rho_{\text{bcp}} = -0.26\text{--}(-0.27) \text{ he}^{-1}$) and even more ionic Al–C_{NHC} ($G/\rho_{\text{bcp}} = 1.08\text{--}1.13 \text{ he}^{-1}$, $H/\rho_{\text{bcp}} = -0.23\text{--}(-0.24) \text{ he}^{-1}$) bond. Noteworthy, G/ρ_{bcp} of M–C_{NHC} (M = Al, Ga, In) bonds follow the trend of Pauling electronegativity differences, which decrease in the order Al–C_{NHC} (0.94) > In–C_{NHC} (0.77) > Ga–C_{NHC} (0.74), similarly to X₃ADY₃ (A = B, Al; D = N, P) recently discussed by Mebs and Beckmann.^{36b} Interestingly, the differences of H/ρ_{bcp} for M–C_{NHC} (M = Al, Ga, In) followed electronegativity differences, taking into account the Allred and Rochow electronegativity scale (Al–C_{NHC} (1.03) \approx In–C_{NHC} (1.01) > Ga–C_{NHC} (0.68)). As a result, ionicity and covalency of M–C_{NHC} bonds could be better described by Allen electronegativity differences, which decrease in the order Al–C_{NHC} (0.931) > In–C_{NHC} (0.888) > Ga–C_{NHC} (0.788).⁴⁰ Consistently, in the case of Me₂MOR(NHC) (NHC = IMes, SIMes), the Raub–Jansen indexes (RJIs)⁴¹ of Ga–C_{NHC} (86–88%) were significantly lower in comparison with In–C_{NHC} (89–90%) and mainly ionic Al–C_{NHC} (95%) bonds. The difference between the mainly ionic Al–C_{NHC} bonds and predominantly polar covalent Ga–C_{NHC} bonds are visible in the ELI-D distribution mapped onto the corresponding bonding basins (Figure 5). The smallest electron-contribution of Al atom in the M–C_{NHC} bond is indicated by the green color area in the direction to the Al atom compared to the blue-color area for In and Ga; however, the In–C_{NHC} basin is flattened in the metal direction. The volumes of the ELI-D basin $V_{001\text{ELI}}$ (cut at 0.001 au), which range from around 9 to 11 Å³,³ are relatively large in comparison with other bonds in the coordination sphere of aluminum gallium and indium. For any series of investigated Me₂MOR(NHC) (M = Al, Ga, In) complexes, smaller volumes were observed in the case of gallium complexes, in comparison with aluminum or indium. Interestingly, significantly smaller volumes were observed for the Me₂MOR(SIMes), as well as Me₂MOR(6-Mes) complexes, with saturated NHCs in comparison with Me₂MOR(IMes) complexes with unsaturated IMes carbene. The latter, which affect the electron density distribution in the vicinity of carbene carbon, could be responsible for a more significant shift of carbene carbon in ¹³C NMR in the case of Me₂MOR(NHC) complexes with saturated NHCs (Table 1). The most striking example includes a larger shift of carbene carbon of Me₂M(OCPh₂Me)(6-Mes) (M = Ga, In) in comparison with Me₂M(OCPh₂Me)(IMes), although a stronger Al–C_{IMes} bond was clearly evidenced by X-ray analysis in the solid state.^{5c}

Although the strength of M–C_{NHC} bonds, determined on the basis of both X-ray analysis calculations of BDEs, could not explain the reactivity of investigated Me₂MOR(NHC) (M = Al, Ga, In; NHC = IMes, SIMes) complexes, the ionic character of M–C_{NHC} bonds, which increased in series: Ga–C_{NHC} < In–C_{NHC} < Al–C_{NHC} could be much more easily associated with the reactivity, including stability, of Me₂MOR(NHC) complexes. With regard to the latter, noteworthy is the reactivity of the Al–C_{NHC} bond of both aluminum alkoxides/aryloxides with NHCs,^{12h} as well as trialkylaluminum NHC adducts,⁴² the latter additionally supported by DFT studies. In the case of the catalytic activity of Me₂MOR(NHC) complexes in ROP, the most polar covalent character of Ga–C_{NHC} was

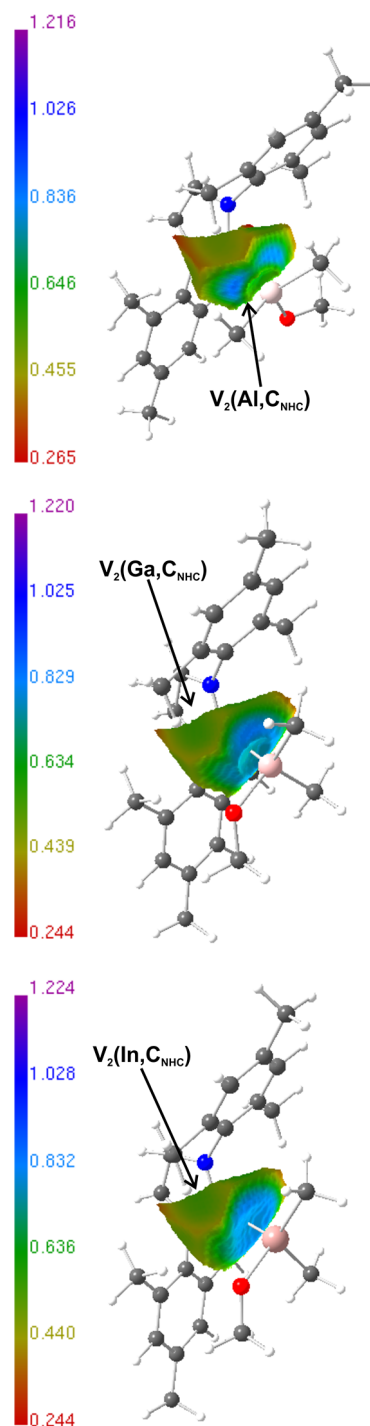


Figure 5. ELI-D distributions onto $V_2(\text{Al}, \text{C}_{\text{NHC}})$, $V_2(\text{Ga}, \text{C}_{\text{NHC}})$, and $V_2(\text{In}, \text{C}_{\text{NHC}})$ bonding (disynaptic valence) basins of **1a**.

intact toward lactide in contrast to In–C_{NHC} and Al–C_{NHC} bonds. The character of M–C_{NHC} (M = Al, Ga, In) bonds was also interesting in the light of the recent debate on the proper Lewis formula representation of donor–acceptor complexes,⁴³ which was recently discussed by Mebs and Beckmann with regard to RSBI of A–D bonds of X₃ADY₃ (A = B, Al; D = N, P) complexes.^{36b} For discussed Me₂MOR(NHC) complexes, both structure/reactivity studies and calculations concerning Me₂MOR(NHC) complexes suggest the dominating canonical form for Ga–C_{NHC} and arrow notation for Al–C_{NHC} bonds, In

the case of $\text{In}-\text{C}_{\text{NHC}}$, a combination of these two notations would be much more suitable.

CONCLUSIONS

We have focused on the effect of group 13 metals on the synthesis, structure, and reactivity of $\text{Me}_2\text{MOR}(\text{NHC})$ ($\text{M} = \text{Al}, \text{Ga}, \text{In}$) complexes, with regard to the strength and character of $\text{M}-\text{C}_{\text{NHC}}$ bonds. Therefore, we have investigated the effect of alkoxide ligands and NHCs on the formation, stability, and structure of $\text{Me}_2\text{AlOR}(\text{NHC})$ alkoxides, as well as and their reactivity, including catalytic activity in the ring-opening polymerization (ROP) of lactide, in comparison with their gallium and indium analogues that have been already reported by us. The synthesis of $\text{Me}_2\text{AlOR}(\text{NHC})$, and the formation of $\text{Al}-\text{C}_{\text{NHC}}$ bond, with aluminum possessing a smaller radius in comparison with gallium and indium, is strongly dependent on the accessibility of the fifth coordinate site of aluminum in $[\text{Me}_2\text{Al}(\mu\text{-OR})]_n$ ($n = 2, 3$) aggregates. However, the structure of the resulting $\text{Me}_2\text{AlOR}(\text{NHC})$ complexes, their stability or tendency for ligand disproportionation, as well as reactivity toward lactide in the ROP, is strongly dependent on both the strength and character of $\text{Al}-\text{C}_{\text{NHC}}$ bonds, rather than only their strength, as we suggested previously for $\text{Me}_2\text{MOR}(\text{NHC})$ ($\text{M} = \text{Ga}, \text{In}$) complexes. While the strength of $\text{M}-\text{C}_{\text{NHC}}$ bonds was determined using spectroscopic techniques, as well as calculations of their bond dissociation energies (BDEs), real-space bonding indicators (RSBIs), obtained from density functional theory (DFT) calculations and topological analysis of the computed electron and pair densities according to the atoms-in-molecules (AIM) and electron localizability indicator (ELI-D) space partitioning schemes, were used for the determination of the character of $\text{M}-\text{C}_{\text{NHC}}$ bonds of $\text{Me}_2\text{MOR}(\text{NHC})$ ($\text{M} = \text{Al}, \text{Ga}, \text{In}$) complexes. The character of $\text{M}-\text{C}_{\text{NHC}}$ bonds, changing from polar covalent in the case $\text{Ga}-\text{C}_{\text{NHC}}$ bonds to essentially only ionic for $\text{Al}-\text{C}_{\text{NHC}}$ bonds (polar covalent character: $\text{Ga}-\text{C}_{\text{NHC}} > \text{In}-\text{C}_{\text{NHC}} > \text{Al}-\text{C}_{\text{NHC}}$) much better reflects the properties of $\text{Me}_2\text{MOR}(\text{NHC})$ complexes than the strength of $\text{M}-\text{C}_{\text{NHC}}$ bonds determined either by spectroscopic techniques or DFT calculations of bond dissociation energies (BDEs). Our studies not only show the important role of the character of the $\text{M}-\text{C}_{\text{NHC}}$ bond on the properties, including catalytic properties of metal NHC complexes, but also confirm that the character of $\text{M}-\text{C}_{\text{NHC}}$ can be estimated using RSBIs.

EXPERIMENTAL SECTION

General Procedures. All operations were carried out under dry argon using standard Schlenk techniques or in a glovebox (MBraun, UniLab). Solvents and reagents were purified and dried prior to use. Solvents were purified using MBRAUN Solvent Purification Systems (MB-SPS-800) and stored over molecular sieves. Deuterated solvents were either dried over potassium (toluene- d_8 , THF- d_6) or calcium hydride (CD_2Cl_2). *rac*-Lactide was purchased from Sigma-Aldrich and further purified by crystallization from anhydrous toluene and sublimation. (*S*)-Methyl lactate, 2-methoxyethanol, and methanol were purchased from Sigma-Aldrich, dried over molecular sieves, and distilled under argon. 1-Phenylethanol and *o*-methoxyphenol (guaiacol) were purchased from Sigma-Aldrich and dried over molecular sieves. 1,1-Diphenylethanol was purchased from Sigma-Aldrich and used as received. Me_3Al and Me_3Ga and Me_3In were purchased from STREM Chemicals, Inc. and used as received. $\text{Me}_2\text{GaOCH}_2\text{CH}_2\text{OMe}$ (IMes) was synthesized analogously to other dialkylgallium alkoxides (see the Supporting Information).⁵ Me_2InOMe (IMes) was synthesized as described previously,⁶ while crystals suitable for X-ray were obtained

from a toluene solution of the reaction mixture. IMes and SIMes were synthesized as described by us previously.^{5a,b} ^1H and ^{13}C NMR spectra were recorded on an Agilent 400-MR DD2 400 MHz spectrometer with shifts given in ppm according to the deuterated solvent shift. Elemental analysis was performed on a Vario EL III instrument (Heraeus). ROP of *rac*-LA with **1a**, **3a**, **4a**, and **4b** was conducted according to the previously described procedure.^{5a,b,6} Compounds **1a**, **1b**, **3a**, and **4a** were isolated in high yields (see below) and characterized in each case by elemental analysis (EA), NMR spectroscopy, and X-ray analysis. Although obtained EA results are low in carbon by 1.56% (**1a**), 1.57% (**1b**), and 3.71% (**3a**), they are correct with regard to the content of hydrogen and nitrogen, and represent the best values we could obtain experimentally. Compound **2a** was not isolated pure in bulk, as it cocrystallized with free IMes present in solution; however, it could be purified by crystallization, which was evidenced by isolation of monocrystals of **2a** suitable for X-ray analysis. The structure of **2a** was additionally confirmed by ^1H and ^{13}C NMR spectroscopy in the presence of 1 equiv of IMes. Compounds $\text{Me}_2\text{Al}(\text{OCPh}_2\text{Me})$ (SIMes) and $\text{Me}_2\text{Al}(\text{OCPhMeH})$ (IMes) were not isolated; however, their formation and structure were evidenced by ^1H and ^{13}C NMR spectroscopy.

Synthesis of Aluminum, Gallium, and Indium Complexes.

Synthesis of 1a. To a stirred solution of $[\text{Me}_2\text{Al}(\mu\text{-OMe})]_3$ (37 mg, 0.14 mmol) in toluene (2 mL) 2 mL of a toluene solution of IMes (128 mg, 0.42 mmol) was added at room temperature. The resulting solution was stirred for 20 min. Then toluene was removed under a vacuum to give a white crystalline solid, which was recrystallized from toluene/hexane solution at -18°C , and colorless crystals were dried under a vacuum (115 mg, 70%). Anal. Calcd for $\text{C}_{24}\text{H}_{33}\text{AlN}_2\text{O}$: C, 73.44, H, 8.47, N, 7.14. Found: C, 71.88, H, 8.45, N, 6.92. ^1H NMR (toluene- d_8 , 400 MHz): -1.09 (s, 6H, AlCH_3), 2.03 (s, 12H, CH_3), 2.10 (s, 6H, CH_3), 3.38 (s, 3H, OCH_3), 6.18 (br s, 2H, CH), 6.73 (s, 4H, CH_{Ar}). ^{13}C $\{^1\text{H}\}$ NMR (toluene- d_8 , 100 MHz): -9.5 (AlMe_2), 17.6, 21.0, 50.6, 122.6, 129.2, 135.4, 137.4, 139.3.

Synthesis of 1b. To a stirred solution of $[\text{Me}_2\text{Al}(\mu\text{-OMe})]_3$ (30 mg, 0.11 mmol) in toluene (2 mL) 2 mL of a toluene solution of SIMes (101 mg, 0.33 mmol) was added at room temperature. The resulting solution was stirred for 20 min. Then toluene was removed under a vacuum to give a white crystalline solid, which was recrystallized from toluene solution at -18°C , and colorless crystals were dried under a vacuum (98.5 mg, 76%). Anal. Calcd for $\text{C}_{24}\text{H}_{35}\text{AlN}_2\text{O}$: C, 73.06, H, 8.94, N, 7.10. Found: C, 71.49, H, 9.05, N, 7.17. ^1H NMR (THF- d_8 , 400 MHz), ^{13}C NMR (THF- d_8 , 100 MHz): dissolving **1b** immediately caused its partial decomposition; in this case signals corresponding to **1b** could not be clearly distinguished (see the Supporting Information).

Synthesis of 2a/IMes. To a stirred solution of $[\text{Me}_2\text{Al}(\mu\text{-OCH}_2\text{CH}_2\text{Me})]_2$ (32 mg, 0.12 mmol) in toluene (4 mL) 2 mL of a toluene solution of IMes (146 mg, 0.48 mmol) was added at room temperature. The resulting solution was stirred for 30 min. Then toluene was removed under a vacuum to give a white crystalline solid of **2a** and IMes. ^1H NMR (toluene- d_8 , 400 MHz): **2a**: -1.12 (s, 6H, AlCH_3), 2.02 (s, 12H, CH_3), 2.09 (s, 6H, CH_3), 3.17 (s, 3H, OCH_3), 3.31 (t, $J = 6.4$ Hz, 2H, CH_2), 3.63 (t, $J = 6.4$ Hz, 2H, CH_2), 6.27 (s, 2H, CH), 6.74 (s, 4H, CH_{Ar}); IMes: 2.04 (s, 12H, CH_3), 2.14 (s, 6H, CH_3), 6.51 (s, 2H, CH), 6.72 (s, 4H, CH_{Ar}). ^{13}C $\{^1\text{H}\}$ NMR (toluene- d_8 , 100 MHz): **2a**: -9.0 (AlMe_2), 17.6, 21.3, 58.4, 62.0, 77.2, 122.8, 129.2, 135.5, 137.7, 139.0, 174.9 ($\text{C}_{\text{carbene}}$); IMes: 18.0, 21.0, 120.6, 129.0, 135.2, 137.1, 139.1, 217.3 ($\text{C}_{\text{carbene}}$).

Synthesis of 3a. The first step involved the synthesis of $[\text{Me}_2\text{Al}(\mu\text{-OCPh}_2\text{Me})]_2$. A stirred solution of Me_3Al (265 mg, 3.68 mmol) in methylene chloride (10 mL) was cooled to -78°C , and a methylene chloride solution (5 mL) of 1,1-diphenylethanol (728 mg, 3.68 mmol) was added dropwise. The cooling bath was removed, and the reaction mixture was warmed slowly to room temperature, while the evolution of gas was observed, and stirred for an additional 1 h. The solvent and volatiles were removed under a vacuum to give a yellowish crystalline solid, which was recrystallized from methylene chloride/hexane at -18°C , and colorless crystals of $[\text{Me}_2\text{Al}(\mu\text{-OCPh}_2\text{Me})]_2$ were dried under a vacuum (749 mg, 80%). ^1H NMR

(toluene- d_8 , 400 MHz): -0.82 (s, 6H, AlCH_3), 2.01 (s, 3H, CH_3), 7.02 – 7.06 (m, 2H, CH_{Ar}), 7.10 – 7.15 (m, 4H, CH_{Ar}), 7.35 – 7.38 (m, 2H, CH_{Ar}). ^{13}C { ^1H } NMR (toluene- d_8 , 100 MHz): -5.7 (AlMe_2), 31.3 , 81.8 , 127.9 , 128.1 , 128.3 , 145.5 . To a stirred solution of $[\text{Me}_2\text{Al}(\mu\text{-OCPh}_2\text{Me})]_2$ (92 mg, 0.18 mmol) in toluene (4 mL) 2 mL of a toluene solution of IMes (109 mg, 0.36 mmol) was added at room temperature. The resulting solution was stirred for 11 days. Then toluene was removed under a vacuum to give a yellowish crystalline solid, which was recrystallized from toluene/hexane solution at -18 °C, and colorless crystals were dried under a vacuum (162 mg, 81%). Anal. Calcd for $\text{C}_{37}\text{H}_{43}\text{AlN}_2\text{O}$: C, 79.54, H, 7.76, N, 5.01. Found: C, 75.83, H, 7.64, N, 4.98. ^1H NMR (toluene- d_8 , 400 MHz): -1.23 (s, 6H, AlCH_3), 1.86 (s, 3H, CH_3), 1.99 (s, 12H, CH_3), 2.14 (s, 6H, CH_3), 5.98 (s, 2H, CH), 6.74 (s, 4H, CH_{Ar}), 7.03 – 7.07 (m, 2H, CH_{Ar}), 7.11 – 7.16 (m, 4H, CH_{Ar}), 7.36 – 7.39 (m, 4H, CH_{Ar}). ^{13}C { ^1H } NMR (toluene- d_8 , 100 MHz): -6.1 (AlMe_2), 17.8 , 21.0 , 32.8 , 76.4 , 122.6 , 125.3 , 127.3 , 127.4 , 129.3 , 135.5 , 135.6 , 139.2 , 153.5 , 175.0 ($\text{C}_{\text{carbene}}$).

Synthesis of $\text{Me}_2\text{Al}(\text{OCPh}_2\text{Me})(\text{SIMes})$. To a stirred solution of $[\text{Me}_2\text{Al}(\mu\text{-OCPh}_2\text{Me})]_2$ (66 mg, 0.13 mmol) in toluene (2 mL) 2 mL of a toluene solution of SIMes (80 mg, 0.26 mmol) was added at room temperature. The resulting solution was stirred for 3 months. Then toluene was removed under a vacuum to give a white crystalline solid, which was recrystallized from a toluene/hexane solution at -18 °C, and colorless crystals were dried under a vacuum. The isolation of pure $\text{Me}_2\text{Al}(\text{OCPh}_2\text{Me})(\text{SIMes})$ was not possible due to cocrystallization of $\text{Me}_2\text{Al}(\text{OCPh}_2\text{Me})(\text{SIMes})$ and SIMes; however, signals corresponding to $\text{Me}_2\text{Al}(\text{OCPh}_2\text{Me})(\text{SIMes})$ could be clearly distinguished. ^1H NMR (toluene- d_8 , 400 MHz): -1.31 (s, 6H, AlCH_3), 1.83 (s, 3H, CH_3), 2.12 (s, 12H, CH_3), 2.18 (s, 6H, CH_3), 3.05 (s, 2H, CH_2), 6.73 (s, 4H, CH_{Ar}), 7.12 – 7.20 (m, 6H, CH_{Ar}), 7.11 – 7.16 (m, 4H, CH_{Ar}), 7.35 – 7.37 (m, 4H, CH_{Ar}). ^{13}C { ^1H } NMR (toluene- d_8 , 100 MHz): -6.0 (AlMe_2), 18.1 , 21.0 , 32.7 , 51.0 , 76.4 , 125.4 , 127.3 , 127.4 , 129.7 , 135.5 , 136.2 , 138.4 , 153.4 , 198.1 ($\text{C}_{\text{carbene}}$).

Synthesis of **4a.** To a stirred suspension of $[\text{Me}_2\text{Al}(\mu\text{-OC}_6\text{H}_4\text{OMe})]_2$ (68 mg, 0.19 mmol) in toluene (10 mL) 2 mL of a toluene solution of IMes (116 mg, 0.38 mmol) were added at room temperature, and the resulting solution was stirred for 0.5 h. Then toluene was removed under a vacuum to give a white crystalline solid, which was recrystallized from toluene/hexane at -18 °C to give white crystals, which were dried under a vacuum (123 mg, 69%). Anal. Calcd for $\text{C}_{30}\text{H}_{37}\text{AlN}_2\text{O}_2$: C, 74.35; H, 7.70; N, 5.78. Found: C, 74.21; H, 7.86; N, 5.54. ^1H NMR (toluene- d_8 , 400 MHz): -1.03 (s, 6H, AlCH_3), 2.08 (s, 6H, CH_3), 2.10 (s, 12H, CH_3), 3.40 (s, 3H, OCH_3), 6.06 (s, 2H, CH), 6.57 (dd, 1H, $J = 7.9$, 1.7 Hz, CH_{Ar}), 6.62 (dd, 1H, $J = 7.3$, 1.6 Hz, CH_{Ar}), 6.68 (s, 4H, CH_{Ar}), 6.72 (dd, 1H, $J = 7.9$, 1.6 Hz, CH_{Ar}), 6.84 – 6.90 (m, 1H, CH_{Ar}). ^{13}C { ^1H } NMR (toluene- d_8 , 100 MHz): -8.2 (AlMe_2), 17.6 , 21.0 , 54.6 , 111.7 , 116.1 , 119.9 , 121.4 , 122.6 , 129.3 , 135.4 , 139.2 , 151.0 , 152.3 , 175.5 ($\text{C}_{\text{carbene}}$).

Synthesis of **4b.** To a suspension of $[\text{Me}_2\text{Al}(\mu\text{OC}_6\text{H}_4\text{OMe})]_2$ (54 mg, 0.15 mmol) in toluene (10 mL) 2 mL of a toluene solution of IMes (91 mg, 0.30 mmol) was added at room temperature, and the resulting solution was stirred for 0.5 h. Then toluene was removed under a vacuum to give a white crystalline solid, which was recrystallized from toluene at -18 °C to give white crystals, which were dried under a vacuum (92 mg, 63%). Anal. Calcd for $\text{C}_{30}\text{H}_{39}\text{AlN}_2\text{O}_2$: C, 74.05; H, 8.08; N, 5.76. Found: C, 74.13; H, 8.07; N, 5.72. ^1H NMR (toluene- d_8 , 400 MHz): -1.14 (s, 6H, AlCH_3), 2.05 (s, 6H, CH_3), 2.29 (s, 12H, CH_3), 3.16 (s, 4H, CH_2), 3.35 (s, 3H, OCH_3), 6.51 (dd, 1H, $J = 7.9$, 1.6 Hz, CH_{Ar}), 6.60 (td, 1H, $J = 7.6$, 1.6 Hz, CH_{Ar}), 6.67 (s, 4H, CH_{Ar}), 6.71 (dd, 1H, $J = 7.9$, 1.6 Hz, CH_{Ar}), 6.85 (td, 1H, $J = 7.6$, 1.7, CH_{Ar}). ^{13}C { ^1H } NMR (toluene- d_8 , 100 MHz): -8.1 (AlMe_2), 17.9 , 21.0 , 51.1 , 54.5 , 111.6 , 116.1 , 118.9 , 121.3 , 129.7 , 135.4 , 136.2 , 138.3 , 151.0 , 152.1 , 198.6 ($\text{C}_{\text{carbene}}$).

X-ray Structure Determination. Single crystals suitable for X-ray diffraction studies were selected under a polarizing microscope, mounted in inert oil and transferred to the cold gas stream of the diffractometer. Diffraction data were measured with graphite-monochromated $\text{MoK}\alpha$ ($\lambda = 0.71073$) radiation on the Oxford

Diffraction κ -CCD Gemini A Ultra diffractometer. Cell refinement and data collection as well as data reduction and analysis were performed with the CRYSTALIS^{PRO} software.⁴⁴ Using Olex2,⁴⁵ the structure was solved with the ShelXT⁴⁶ structure solution program using Intrinsic Phasing and refined with the SHELXL program refinement package,⁴⁷ using Least Squares minimization. The crystal data and experimental parameters are summarized in Table S1. Hydrogen atoms were added to the structure model at a geometrically idealized coordinates and refined as riding atoms. CCDC 1852729–1852732 and 1852735–1852737 contain the supplementary crystallographic data for this paper. These data can be obtained free of charge from The Cambridge Crystallographic Data Centre via www.ccdc.cam.ac.uk/data > request/cif.

Crystal Data for **1a.** $\text{C}_{24}\text{H}_{33}\text{N}_2\text{OAl}$ ($M = 392.50$ g/mol): monoclinic, $P2_1/n$, $a = 7.8428(2)$ Å, $b = 23.1863(5)$ Å, $c = 12.5518(4)$ Å, $\beta = 92.450(2)^\circ$, $V = 2280.40(11)$ Å³, $Z = 4$, $T = 120.0(1)$ K, $\mu(\text{MoK}\alpha) = 0.105$ mm⁻¹, 36 935 reflections measured ($6.964^\circ \leq 2\theta \leq 53.74^\circ$), 4886 unique ($R_{\text{int}} = 0.0517$, $R_{\text{sigma}} = 0.0286$) which were used in all calculations. The final R_1 was 0.0405 ($I > 2\sigma(I)$) and wR_2 was 0.1088 (all data).

Crystal Data for **1b.** $\text{C}_{24}\text{H}_{35}\text{AlN}_2\text{O}$ ($M = 394.52$ g/mol): orthorhombic, $Pna2_1$, $a = 22.7296(11)$ Å, $b = 7.9504(4)$ Å, $c = 13.1086(10)$ Å, $V = 2368.8(2)$ Å³, $Z = 4$, $T = 293(1)$ K, $\mu(\text{MoK}\alpha) = 0.101$ mm⁻¹, 15287 reflections measured ($6.984^\circ \leq 2\theta \leq 52.246^\circ$), 4667 unique ($R_{\text{int}} = 0.0406$, $R_{\text{sigma}} = 0.0462$) which were used in all calculations. The final R_1 was 0.0447 ($I > 2\sigma(I)$) and wR_2 was 0.1116 (all data).

Crystal Data for **2a.** $\text{C}_{26}\text{H}_{37}\text{N}_2\text{O}_2\text{Al}$ ($M = 436.55$ g/mol): triclinic, P , $a = 8.1815(4)$ Å, $b = 8.5023(4)$ Å, $c = 19.5640(7)$ Å, $\alpha = 94.985(4)^\circ$, $\beta = 91.892(4)^\circ$, $\gamma = 107.000(4)^\circ$, $V = 1294.07(10)$ Å³, $Z = 2$, $T = 120.0(1)$ K, $\mu(\text{MoK}\alpha) = 0.101$ mm⁻¹, 11 113 reflections measured ($6.87^\circ \leq 2\theta \leq 51.75^\circ$), 4995 unique ($R_{\text{int}} = 0.0304$, $R_{\text{sigma}} = 0.0440$) which were used in all calculations. The final R_1 was 0.0501 ($I > 2\sigma(I)$) and wR_2 was 0.1320 (all data).

Crystal Data for **3a.** $\text{C}_{37}\text{H}_{43}\text{N}_2\text{OAl}$ ($M = 558.71$ g/mol): triclinic, P , $a = 9.9657(8)$ Å, $b = 10.4394(7)$ Å, $c = 17.1951(13)$ Å, $\alpha = 82.894(6)^\circ$, $\beta = 81.462(7)^\circ$, $\gamma = 72.973(7)^\circ$, $V = 1685.4(2)$ Å³, $Z = 2$, $T = 293.1(2)$ K, $\mu(\text{MoK}\alpha) = 0.089$ mm⁻¹, 18 014 reflections measured ($6.722^\circ \leq 2\theta \leq 52.114^\circ$), 6638 unique ($R_{\text{int}} = 0.0474$, $R_{\text{sigma}} = 0.0583$) which were used in all calculations. The final R_1 was 0.0514 ($I > 2\sigma(I)$) and wR_2 was 0.1450 (all data).

Crystal Data for **4a.** $\text{C}_{30}\text{H}_{37}\text{AlN}_2\text{O}_2$ ($M = 484.59$ g/mol): triclinic, P , $a = 7.6209(3)$ Å, $b = 8.4804(3)$ Å, $c = 23.5527(7)$ Å, $\alpha = 82.549(2)^\circ$, $\beta = 86.426(3)^\circ$, $\gamma = 64.056(4)^\circ$, $V = 1357.18(9)$ Å³, $Z = 2$, $T = 120.0(1)$ K, $\mu(\text{MoK}\alpha) = 0.103$ mm⁻¹, 22 514 reflections measured ($6.876^\circ \leq 2\theta \leq 54.34^\circ$), 5997 unique ($R_{\text{int}} = 0.0260$, $R_{\text{sigma}} = 0.0192$) which were used in all calculations. The final R_1 was 0.0393 ($I > 2\sigma(I)$) and wR_2 was 0.1099 (all data).

Computational Methodology (BDEs). The geometry optimization of all studied systems were carried out at the ω B97X-D level of theory using the 6-311++G** triple- ζ basis set for all atoms except In, for which we used def2-ECP basis set.⁴⁸ The input coordinates were generated from the X-ray single-crystal data. BDE was defined as the difference between the energy of the complex and the sum of the energy of the carbene and the remaining part of the complex. For DFT calculations, we used the Boys–Bernardi counterpoise scheme to correct for the basis set superposition error.⁴⁹ All DFT calculations were performed in the Gaussian09 program.⁵⁰ We also performed single-point DLPNO–CCSD(T)⁵¹ energy calculations in the def2-svp basis set using the Orca v4.0.0.1 program⁵² and used it independently to estimate BDEs.

Computational Methodology (RSBIs). The single-point calculations of $\text{Me}_2\text{MOMe}(\text{IMes})$ ($M = \text{Al}$ (**1a**), Ga, In), $\text{Me}_2\text{MOMe}(\text{SIMes})$ ($M = \text{Al}$ (**1b**), Ga, In), $\text{Me}_2\text{M}(\text{OCPh}_2\text{Me})(\text{IMes})$ ($M = \text{Al}$ (**3a**), Ga, In), $\text{Me}_2\text{M}(\text{OCPh}_2\text{Me})(6\text{-Mes})$ ($M = \text{Ga}$, In), $\text{Me}_2\text{M}(\text{OC}_6\text{H}_4\text{OMe})(\text{IMes})$ ($M = \text{Al}$ (**4a**), Ga, In) were carried out at the B3PW91 level of theory,⁵³ using effective core potentials for In⁵⁴ along with the associated triple- ζ basis sets⁵⁵ and the 6-311+G(2df,p) basis set for all other atoms. The input coordinates were generated from the X-ray single-crystal data. The distances to hydrogen atoms

were elongated to mean values from neutron-diffraction experiments.⁵⁶ All computations were performed by using the Gaussian09 program.⁵⁰ Subsequently, topological and integrated AIM and ELI-D parameters were derived using AIMAll⁵⁷ and DGID-4.6⁵⁸ on the basis of wave function and checkpoint files, respectively. For the grid calculations, a step size of 0.05 bohr was applied. All molecular graphs are AIMAll representations. ELI-D graphs were shown with MOLISO⁵⁹ with all protonated basins (H atoms) in transparent mode for clarity reasons.

■ ASSOCIATED CONTENT

● Supporting Information

The Supporting Information is available free of charge on the ACS Publications website at DOI: 10.1021/acs.organomet.8b00570.

NMR spectra. Bond valence vector and bond valencies for **3a**. Calculated bond topological and integrated bond descriptors, molecular graphs, isosurface representations of the localization domains of the ELI-D, ELI-D distributions onto $V_2(M, C_{\text{NHC}})$ bonding (disynaptic valence) basins of $\text{Me}_2\text{MOMe}(\text{IMes})$ ($M = \text{Al}$ (**1a**), Ga, In), $\text{Me}_2\text{MOMe}(\text{SIMes})$ ($M = \text{Al}$ (**1b**), Ga, In), $\text{Me}_2\text{M}(\text{OCPh}_2\text{Me})(\text{IMes})$ ($M = \text{Al}$ (**3a**), Ga, In), $\text{Me}_2\text{M}(\text{OCPh}_2\text{Me})(6\text{-Mes})$ ($M = \text{Ga}$, In), $\text{Me}_2\text{M}(\text{OC}_6\text{H}_4\text{OMe})(\text{IMes})$ ($M = \text{Al}$ (**4a**), Ga, In) (PDF)

Accession Codes

CCDC 1852729–1852732 and 1852735–1852737 contain the supplementary crystallographic data for this paper. These data can be obtained free of charge via www.ccdc.cam.ac.uk/data_request/cif, or by emailing data_request@ccdc.cam.ac.uk, or by contacting The Cambridge Crystallographic Data Centre, 12 Union Road, Cambridge CB2 1EZ, UK; fax: +44 1223 336033.

■ AUTHOR INFORMATION

Corresponding Authors

*(P.H.) E-mail: phoreglad@uw.edu.pl. Tel. +48 22 5543670.

*(L.C.) E-mail: lilianna.checinska@chemia.uni.lodz.pl. Tel. +48 42 6354273.

ORCID

Maciej Dranka: 0000-0003-0987-5762

Lilianna Chęcińska: 0000-0002-3546-920X

Paweł Horeglad: 0000-0002-2813-1251

Notes

The authors declare no competing financial interest.

■ ACKNOWLEDGMENTS

This work was financially supported by the National Science Centre of Poland (SONATA BIS2 Programme, Grant No. DEC-2012/07/E/ST5/02860). The authors thank Dr. Łukasz Dobrzycki from University of Warsaw for help with X-ray measurements of $\text{Me}_2\text{InOMe}(\text{IMes})$, Prof. Janusz Zachara from Warsaw University of Technology for calculations of the resultant bond valence vector of **3a** and helpful discussions, and Dr. Andrzej Plichta from Warsaw University of Technology for GPC measurements. TOC/abstract artwork was done by Anna Maria Dąbrowska (full.nonmetal.chemist@gmail.com).

■ REFERENCES

(1) (a) Willans, C. E. *Organometallic Chemistry*; The Royal Society of Chemistry: London, 2010; Vol. 36, pp 1–28. (b) Hudnall, T. W.;

Ugarte, R. A.; Perera, T. A. Main Group Complexes with N-Heterocyclic Carbenes: Bonding, Stabilization and Applications in Catalysis. In *N-Heterocyclic Carbenes: From Laboratory Curiosities to Efficient Synthetic Tools*; Diez-González, S., Ed.; RSC Catalysis Series No. 27; The Royal Society of Chemistry, 2017; pp 178–237. (c) Nesterov, V.; Reiter, D.; Bag, P.; Frisch, P.; Holzner, R.; Porzelt, A.; Inoue, S. *Chem. Rev.* **2018**, *118*, 9678–9842.

(2) See the representative reviews on NHC complexes of: group 13 metals (a) Fliedel, C.; Schnee, G.; Avilés, T.; Dagorne, S. *Coord. Chem. Rev.* **2014**, *275*, 63–86. group 1 and 2 metals - (b) Bellemin-Lapponnaz, S.; Dagorne, S. *Chem. Rev.* **2014**, *114*, 8747–8774.

(3) Byers, J. A.; Biernesser, A. B.; Delle Chiaie, K. R.; Kaur, A.; Kehl, J. A. *Adv. Polym. Sci.* **2017**, *279*, 67–118.

(4) Romain, C.; Fliedel, C.; Bellemin-Lapponnaz, S.; Dagorne, S. *Organometallics* **2014**, *33*, 5730–5739.

(5) (a) Horeglad, P.; Szczepaniak, G.; Dranka, M.; Zachara, J. *Chem. Commun.* **2012**, *48*, 1171–1173. (b) Horeglad, P.; Cybularczyk, M.; Trzaskowski, B.; Zukowska, G. Z.; Dranka, M.; Zachara, J. *Organometallics* **2015**, *34*, 3480–3496. (c) Cybularczyk-Cecotka, M.; Dąbrowska, A. M.; Guńka, P. A.; Horeglad, P. *Inorganics* **2018**, *6*, 28.

(6) Cybularczyk, M.; Dranka, M.; Zachara, J.; Horeglad, P. *Organometallics* **2016**, *35*, 3311–3322.

(7) Arnold, P. L.; Casely, I. J.; Turner, Z. R.; Bellabarba, R.; Tooze, R. B. *Dalton Trans.* **2009**, 7236–7247.

(8) (a) Jensen, T. R.; Breyfogle, L. E.; Hillmyer, M. A.; Tolman, W. B. *Chem. Commun.* **2004**, 2504–2505. (b) Wang, D.; Wurst, K.; Buchmeiser, M. R. *J. Organomet. Chem.* **2004**, *689*, 2123–2130. (c) Jensen, T. R.; Schaller, C. P.; Hillmyer, M. A.; Tolman, W. B. *J. Organomet. Chem.* **2005**, *690*, 5881–5891. (d) Fliedel, C.; Mameri, S.; Dagorne, S.; Avilés, T. *Appl. Organomet. Chem.* **2014**, *28*, 504–511. (e) Fliedel, C.; Vila-Viçosa, D.; Calhorda, M. J.; Dagorne, S.; Avilés, T. *ChemCatChem* **2014**, *6*, 1357–1367.

(9) Schnee, G.; Bolley, A.; Hild, F.; Specklin, D.; Dagorne, S. *Catal. Today* **2017**, *289*, 204–210.

(10) Schnee, G.; Bolley, A.; Gourlaouen, C.; Welter, R.; Dagorne, S. *J. Organomet. Chem.* **2016**, *820*, 8–13.

(11) Specklin, D.; Fliedel, C.; Gourlaouen, C.; Bruyere, J.-C.; Avilés, T.; Boudon, C.; Ruhlmann, L.; Dagorne, S. *Chem. - Eur. J.* **2017**, *23*, 5509–5519.

(12) For the representative examples of main group metal alkoxides and aryloxides see group 1: (a) Arnold, P. L.; Rodden, M.; Davis, K. M.; Scarisbrick, A. C.; Blake, A. J.; Wilson, C. *Chem. Commun.* **2004**, 1612–1613. (b) Arnold, P. L.; Rodden, M.; Wilson, C. *Chem. Commun.* **2005**, 1743–1745. (c) Zhang, D.; Kawaguchi, H. *Organometallics* **2006**, *25*, 5506–5509. (d) Yao, H.; Zhang, J.; Zhang, Y.; Sun, H.; Shen, Q. *Organometallics* **2010**, *29*, 5841–5846. (e) Arnold, P. L.; Turner, Z. R.; Bellabarba, R.; Tooze, R. P. *J. Am. Chem. Soc.* **2011**, *133*, 11744–11756. Group 2: see ref 7 and 12c. Group 12: see ref 8 (f) Anantharaman, G.; Elango, K. *Organometallics* **2007**, *26*, 1089–1092. (g) Jochmann, P.; Stephan, D. W. *Chem. - Eur. J.* **2014**, *20*, 8370–8378. group 13: see ref 4–6 (h) Dardun, V.; Escomel, L.; Jeanneau, E.; Camp, C. *Dalton Trans.* **2018**, *47*, 10429–10433. group 14: (i) Rupa, P. A.; Jennings, M. C.; Baines, K. M. *Organometallics* **2008**, *27*, 5043–5051. (j) Ruddy, A. J.; Rupa, P. A.; Bladek, K. J.; Allan, C. J.; Avery, J. C.; Baines, K. M. *Organometallics* **2010**, *29*, 1362–1367. (k) Rupa, P. A.; Staroverov, V. N.; Baines, K. M. *Organometallics* **2010**, *29*, 4871–4881. (l) Paul, D.; Heins, F.; Krupski, S.; Hepp, A.; Daniliuc, C. G.; Klahr, K.; Neugebauer, J.; Glorius, F.; Hahn, E. *Organometallics* **2017**, *36*, 1001–1008.

(13) Silva Valverde, M. F.; Schweyen, P.; Gisinger, D.; Bannenberg, T.; Freytag, M.; Kleeberg, C.; Tamm, M. *Angew. Chem., Int. Ed.* **2017**, *56*, 1135–1140.

(14) (a) Tan, G.; Szilvási, T.; Inoue, S.; Blom, B.; Driess, M. *J. Am. Chem. Soc.* **2014**, *136*, 9732–9742. (b) Li, B.; Kundu, S.; Stückl, A. C.; Zhu, H.; Keil, H.; Herbst-Irmer, R.; Stalke, D.; Schwederski, B.; Kaim, W.; Andradá, D. M.; Frenking, G.; Roesky, H. *Angew. Chem., Int. Ed.* **2017**, *56*, 397–400.

- (15) Higelin, A.; Keller, S.; Göhringer, C.; Jones, C.; Krossing, I. *Angew. Chem., Int. Ed.* **2013**, *52*, 4941–4944.
- (16) Wu, M. M.; Gill, A. M.; Yunpeng, L.; Yongxin, L.; Ganguly, R.; Falivene, L.; Garcia, F. *Dalton Trans.* **2017**, *46*, 854–864.
- (17) The tilt is quantified by the offset angle of the M–C bond to the C2 axis of the NHC, which is split into pitch and yaw angles. See for example: (a) Arnold, P. L.; Liddle, S. T. *Chem. Commun.* **2006**, 3959–3971. (b) Higelin, A.; Keller, S.; Göhringer, C.; Jones, C.; Krossing, I. *Angew. Chem., Int. Ed.* **2013**, *52*, 4941–4944.
- (18) Arduengo, A. J.; Dias, H. V.R.; Harlow, R. L.; Kline, M. J. *Am. Chem. Soc.* **1992**, *114*, 5530–5534.
- (19) Arduengo, A. J.; Goerlich, J. R.; Marshall, W. J. *J. Am. Chem. Soc.* **1995**, *117*, 11027–11028.
- (20) For structural and spectroscopic evidence of the formation of M–C_{NHC} complexes, see: Dröge, T.; Glorius, F. *Angew. Chem., Int. Ed.* **2010**, *49*, 6940–6953.
- (21) Brown, I. D.; Altermatt, D. *Acta Crystallogr., Sect. B: Struct. Sci.* **1985**, *41*, 244–247.
- (22) Dąbrowska, A. M.; Hurko, A.; Dranka, M.; Varga, V.; Urbańczyk, M.; Horeglad, P. *J. Organomet. Chem.* **2017**, *840*, 63–69.
- (23) Lewiński, J.; Zachara, J.; Justyniak, I. *Chem. Commun.* **1997**, 1519–1520.
- (24) Horeglad, P.; Kruk, P.; Pécaut, J. *Organometallics* **2010**, *29*, 3729–3734.
- (25) Horeglad, P.; Cybularczyk, M.; Litwińska, A.; Dąbrowska, A. M.; Dranka, M.; Zukowska, G. Z.; Urbańczyk, M.; Michalak, M. *Polym. Chem.* **2016**, *7*, 2022–2036.
- (26) Lewiński, J.; Zachara, J.; Justyniak, I. *Chem. Commun.* **2002**, 1586–1587.
- (27) Lewiński, J.; Zachara, J.; Justyniak, I. *Organometallics* **1997**, *16*, 4597–4605.
- (28) Lewiński, J.; Horeglad, P.; Wójcik, K.; Justyniak, I. *Organometallics* **2005**, *24*, 4588–4593.
- (29) Lewiński, J.; Zachara, J.; Gos, P.; Grabska, E.; Kopec, T.; Madura, I.; Marciniak, W.; Prowotorow, I. *Chem. - Eur. J.* **2000**, *6*, 3215–3227.
- (30) For the discussion on the nature of CH...HC interactions see: Danovich, D.; Shaik, S.; Neese, F.; Echeverría, J.; Aullón, G.; Alvarez, S. *J. Chem. Theory Comput.* **2013**, *9*, 1977–1991.
- (31) Zachara, J. *Inorg. Chem.* **2007**, *46*, 9760–9767.
- (32) For the discussion on the use of bond valence vector (BVV) for the determination of constraints within metal coordination sphere see: Horeglad, P.; Abilimov, O.; Szczepaniak, G.; Dąbrowska, A. M.; Dranka, M.; Zachara, J. *Organometallics* **2014**, *33*, 100–111.
- (33) Dove, A. P.; Li, H.; Pratt, R. C.; Lohmeijer, B. G.G.; Culkun, D. A.; Waymouth, R. M.; Hedrick, J. L. *Chem. Commun.* **2006**, 2881.
- (34) Bader, R. F. W. *Atoms in Molecules. A Quantum Theory*; Oxford University Press: Oxford, U.K., 1990.
- (35) (a) Kohout, M. *Int. J. Quantum Chem.* **2004**, *97*, 651–658. (b) Kohout, M.; Wagner, F. R.; Grin, Y. *Theor. Chem. Acc.* **2008**, *119*, 413–420.
- (36) (a) Hupf, E.; Lork, E.; Mebs, S.; Checińska, L.; Beckmann, J. *Organometallics* **2014**, *33*, 7247–7259. (b) Mebs, S.; Beckmann, J. *J. Phys. Chem. A* **2017**, *121*, 7717–7725. (c) Fugel, M.; Beckmann, J.; Jayatilaka, D.; Gibbs, G. V.; Grabowsky, S. *Chem. - Eur. J.* **2018**, *24*, 6248–6261.
- (37) Mebs, S.; Chilleck, M. A.; Grabowsky, S.; Braun, T. *Chem. - Eur. J.* **2012**, *18*, 11647–11661.
- (38) Pushkarevsky, N. A.; Petrov, P. A.; Grigoriev, D. S.; Smolentsev, A. I.; Lee, L. M.; Kleemiss, F.; Salnikov, G. E.; Konchenko, S. N.; Vargas-Baca, I.; Grabowsky, S.; Beckmann, J.; Zibarev, A. V. *Chem. - Eur. J.* **2017**, *23*, 10987–10991.
- (39) The X-ray structures of Me₂M(OC₆H₄OMe)(IMes) (M = Ga, In) are thoroughly discussed in another article (in preparation), and therefore they were only used for DFT calculations.
- (40) Allen, L. C. *J. Am. Chem. Soc.* **1989**, *111*, 9003–9014.
- (41) Raub, S.; Jansen, G. *Theor. Chem. Acc.* **2001**, *106*, 223–232.
- (42) (a) Schnee, G.; Faza, O. N.; Specklin, D.; Jacques, B.; Karmazin, L.; Welter, R.; López, C. S.; Dagorne, S. *Chem. - Eur. J.* **2015**, *21*, 17959–17972. (b) Schnee, G.; Specklin, D.; Djukic, J.-P.; Dagorne, S. *Organometallics* **2016**, *35*, 1726–1734.
- (43) (a) Himmel, D.; Krossing, I.; Schnepf, A. *Angew. Chem., Int. Ed.* **2014**, *53*, 370–374. (b) Frenking, G. *Angew. Chem., Int. Ed.* **2014**, *53*, 6040–6046. (c) Himmel, D.; Krossing, I.; Schnepf, A. *Angew. Chem., Int. Ed.* **2014**, *53*, 6047–6048.
- (44) CRYSLIS^{PRO} Software System; Rigaku: Oxford, UK, 2016.
- (45) Dolomanov, O. V.; Bourhis, L. J.; Gildea, R. J.; Howard, J. A.K.; Puschmann, H. *J. Appl. Crystallogr.* **2009**, *42*, 339–341.
- (46) Sheldrick, G. M. *Acta Crystallogr., Sect. A: Found. Adv.* **2015**, *71*, 3–8.
- (47) Sheldrick, G. M. *Acta Crystallogr., Sect. C: Struct. Chem.* **2015**, *71*, 3–8.
- (48) Chai, J.-D.; Head-Gordon, M. *Phys. Chem. Chem. Phys.* **2008**, *10*, 6615–6620.
- (49) Boys, S. F.; Bernardi, F. *Mol. Phys.* **1970**, *19*, 553–566.
- (50) *Gaussian09, Revision D.01*; Gaussian, Inc.: Wallingford, CT, USA, 2013.
- (51) Riplinger, C.; Neese, G. *J. Chem. Phys.* **2013**, *138*, 034106.
- (52) Neese, F. *Wiley Interdiscip. Rev.: Comput. Mol. Sci.* **2012**, *2*, 73–78.
- (53) (a) Perdew, J. P.; Chevary, J. A.; Vosko, S. H.; Jackson, K. A.; Pederson, M. R.; Singh, D. J.; Fiolhais, C. *Phys. Rev. B: Condens. Matter Mater. Phys.* **1992**, *46*, 6671–6687. (b) Becke, A. D. *J. Chem. Phys.* **1993**, *98*, 5648–5652.
- (54) Metz, B.; Stoll, H.; Dolg, M. *J. Chem. Phys.* **2000**, *113*, 2563–2569.
- (55) Peterson, K. A. *J. Chem. Phys.* **2003**, *119*, 11099–11112.
- (56) Allen, F. H.; Bruno, I. J. *Acta Crystallogr., Sect. B: Struct. Sci.* **2010**, *66*, 380–386.
- (57) Keith, T. A. *AIMAll, TK Gristmill Software*; Overland Park KS, USA, 2014 (aim.tkgristmill.com).
- (58) Kohout, M. *DGRID-4.6*; Radebeul, 2011.
- (59) Hübschle, C. B.; Luger, P. *J. Appl. Crystallogr.* **2006**, *39*, 901–904.